The Decay Rates of Ps Species and Bound Muon to Bound Electron Decay Behaviour

by

Md Samiur Rahman Mir

A thesis submitted in partial fulfillment of the requirements for the degree of

Master of Science

Department of Physics

University of Alberta

Abstract

This study of bound states composed of short-lived particles (i.e., positron and muon) serves a common purpose to describe their bound properties precisely. The calculation of a scattering amplitude can be lengthy and cumbersome when we have a specific spin preference and many Feynman diagrams. We introduce a simple technique of constructing matrices from the spinor product in the amplitudes that can reduce the number of terms saving a significant amount of time. The decay rates of positronium atom and positronium ion have been reproduced to verify this method. The decay rate of the two-photon annihilation of di-positronium molecule is also calculated for the first time including all contributions from the tree level Feynman diagrams. On the other hand, neutrino oscillation has motivated physicists to look for charged lepton flavor violation (CLFV). The Standard Model prediction for CLFV is too small to detect in an experiment; thus any trace of this violation will require new physics. One of the important backgrounds of muon-electron conversion is the weak decay in a muonic atom. The bound muon decay rate has been analytically evaluated with approximations when the decay electron is bound in the atom. The decay rate has vanishing features at two extreme points which have been explained.

Preface

Chapter 2 and 3 are the result of close collaboration with Muhammad Mubasher. Prof. Andrzej Czarnecki and Prof. M. Jamil Aslam showed the tree level diagrams for $\mathrm{Ps}^- \to e^-\gamma$ and $\mathrm{Ps}_2 \to \gamma\gamma$. The symmetry factor in Appendix B was derived based on Dr. Wen Chen's note on positronium ion decay and communication with Prof. Andrzej Czarnecki and Prof. M. Jamil Aslam.

Chapter 4 is a review of the search experiments and provides the motivation for bound muon study based on [1, 2, 3]. The asymptotic decay rate ratio for $\gamma \to 1$ (shown in Section 5.3) was derived by Prof. Andrzej Czarnecki first; later I found the ratio for γ near 0 and 1 confirming his result. The procedure of integration in Chapter 5 was devised by me; Prof. Andrzej Czarnecki simplified the final expression with a common factor. The interpretations for vanishing decay ratio developed from the discussions with Prof. Andrzej Czarnecki and Prof. M. Jamil Aslam; my contribution was to find that neutrino wave function suppresses the radial integral in $\mathcal{M}$ when $\gamma \to 1$.

Acknowledgments

First and foremost, I would like to express my sincere gratitude to my supervisor, Prof. Andrzej Czarnecki, for his guidance, encouragement, and advice throughout my M.Sc. study. His regular feedback kept me on track and motivated me in times when I had little progress in research. I have benefited immensely from his constructive remarks and valuable suggestions on honing practical skills for a physicist. I am grateful to Prof. M. Jamil Aslam for teaching me the rudimentary concepts of the bound muon project. Countless stimulating discussions with him gave me the necessary working knowledge for research and shaped my understanding of the thesis topics. I also want to thank Dr. Wen Chen for answering my numerous questions on his note on positronium ion.

I deeply appreciated intriguing discussions with Sneh Modi and Muhammad Mubasher; particularly, I learned many significant features of FORM from these vigorous discussions that helped me in my research. I would like to thank Bo Leng for introducing me to the LyX editor and providing help for writing the thesis. I would also like to show my gratitude to Tahjid Ashfaque for his invaluable technical support when campus IT assistance was unavailable in-person.

I would like to thank my sister, Samia Sultana Mir, and my friends- Azwad Adnan, Raj Shekhar Bose, Faraji Samiul Haque Bijoy, Sebastian Huerta, Maisha Jesmin, Daniel Nisakar, A.O.M. Shamsuddoha, Nancy Xu, and Dr. John Zhang. All of them provided direct and indirect mental support to me during the COVID-19 pandemic; I am indebted to their gesture of kindness at the time of isolation. Lastly, I wish to extend my special thanks to the "International Friendship Group" at the University of Alberta, particularly Ann Siebert and James Siebert for always making me feel welcomed in their community.

Contents

List of Tables

List of Figures

Chapter 1

Introduction

Quantum Electrodynamics (QED) is the quantum theory of the electromagnetic interaction. The notion of antiparticle first emerged from QED in 1930s. A particle and its antiparticle can annihilate each other, also known as the pair annihilation. Positron is the antiparticle of an electron; in other words, it is a positively charged electron. If a proton in an atom is replaced by a positron, the positron will annihilate with one of the bound electrons. Such annihilation is inevitable, since every electron shell has s-orbital ($\ell = 0$) filled out at first, and s-orbital electrons can be found at the point nucleus ($r = 0$ point) because the wave function $\psi_{n,\ell=0}(\boldsymbol{r} = 0) \neq 0$ unlike other orbitals. Thus, an exotic atom is produced which decays into photons and/or another stable atom.

In experiments, a few simple exotic bound states consisting of positrons have been found e.g., positronium (Ps), positronium ion ($Ps^{\pm}$), positronium hydride (PsH), and di-positronium molecule (Ps_2). The calculation for their decay rates up to the leading-order can be performed using QED. As the tree level Feynman diagrams have no loops, there is no divergent integral encountered at this level. Gamma matrix algebra is sufficient to find the corresponding decay rates. The decay rates of Ps, Ps^-, and Ps_2 have been computed in Chapters 2 and 3. We introduce a trick that combines the spinors in the amplitude term and represent the amplitude as a trace of a product of gamma matrices. This makes the calculation much simpler and faster to do. The known decay rates of Ps and Ps^- have been reproduced by this method in Chapter 2. Chapter 3 gives the decay rate of Ps_2 decaying to two photons, which has not been computed considering all Feynman diagram to the leading order until now.

Thanks to the spinor trick we used, these calculations are greatly simplified compared to what had been done previously. For example, sixty-four terms were computed for Ps^- in [4], whereas only eight terms were evaluated for the same problem in Chapter 2. As the number of terms reduces, we can even do the calculation by hand.

Chapter 4 and 5 concerns a problem of bound muon decay. The motivation to explore the decay nature of bound muon decay originates from the search for charged lepton flavor violation. Muon is the optimal particle to exhibit flavor violation due to its various properties (lifetime, production). Neutrino oscillation provides the ground for $\mu - e$ conversion, but the conversion rate according to the Standard Model is largely suppressed by neutrino masses. Therefore, $\mu - e$ conversion rate predicted by the established theory goes beyond the current observation limit. If it is still found in experiments, we will need new physics to answer why the conversion is within the experimental sensitivity. A brief summary of the premise of these experiments is given in Chapter 4.

COMET and Mu2e are two experiments that will search for $\mu - e$ conversion with $\mathcal{O}(10^{-17})$ sensitivity. Since it is a rare process, it is essential to remove any intrinsic background that is in the same order of the conversion. A significant background is muon decay in the atomic orbit. When a muon beam is bombarded on a target, a muonic atom will be formed. The muonic decay into an electron has the same time distribution as the conversion signal. This serves as the motivation to study bound muon decay.

A bound muon can decay into either a free electron or a bound electron. It has been found that the decay probability of a bound electron has larger contribution from the negative energy component of the bound muon state than previously estimated [3]. This surprising discovery calls for a careful investigation on bound-to-bound decay. It is crucial to understand the bound-to-bound decay behaviour to explain the finding of the paper. The decay rate is expressed as a single integral in [3], which is approximately computed in Chapter 5. The decay rate vanishes for both small and large values of atomic number (Z) of the atom, and this property has been explained in that chapter as well.

In summary, this thesis describes Ps species decay and bound muon decay. Although their aspects are different in nature, both projects have a common theme to understand the precise description of bound states governed by QED.

Chapter 2

Decay Rates of Ps and Ps^-

2.1 Introduction

Ps is a two-body bound state of an electron and a positron. Being an antimatter-matter system, this exotic hydrogen-like atom annihilates into photons. Calculation of the decay rate of this two-body system has been performed [5]. It has been of interest to compute decay rates of similar exotic systems consisting of electrons and positrons, that can be found as bound states in Nature. Two examples are $Ps^{\pm}$ and Ps_2. They have been found to exist in experiments [6, 7].

Electron and positron annihilate each other in a Ps atom and converts into photons. However, due to the conservation of 4-momentum, single photon annihilation is not possible for Ps atom. Since $Ps^{\pm}$ has an extra electron (or positron), it can emit a single photon in addition to multi-photon emission from the electron-positron pair annihilation. It motivated physicists to compute this one-photon decay channel for $Ps^{\pm}$. It was done by Kryuchkov [4] for the first time accounting for all Feynman diagrams that contribute in the leading order.

In this chapter, we will reproduce the decay rates of para-positronium and Ps^- using a simple technique by expressing spinors in terms of gamma matrices. We will also explain the symmetry factors due to the identical particles in detail. Using the same mathematical machineries, we will compute the decay rate for Ps_2 in the following chapter.

2.2 Para-positronium Annihilation

The 1s state of Ps atom can decay into photons, where the number of photons depends on the initial spin, S. Thus, the ortho-positronium (o-Ps) ($S = 1$) annihilates into an odd number of photons, while the para-positronium (p-Ps) ($S = 0$) into an even number. This

section will show the calculation of the decay rate of p-Ps into two photons to the leading order of α. We use natural units, $\hbar = c = 1$.

2.2.1 Amplitudes

In p-Ps atom, the electron and the positron can annihilate each other and produce two photons, $e^+e^- \to \gamma\gamma$. Crossing two photons generates two Feynman diagrams as shown in Fig. 2.1. Each diagram for a multi-particle interaction corresponds to a probability amplitude, and observables (e.g., decay rate and scattering cross-section) are computed from the the sum of the amplitudes.

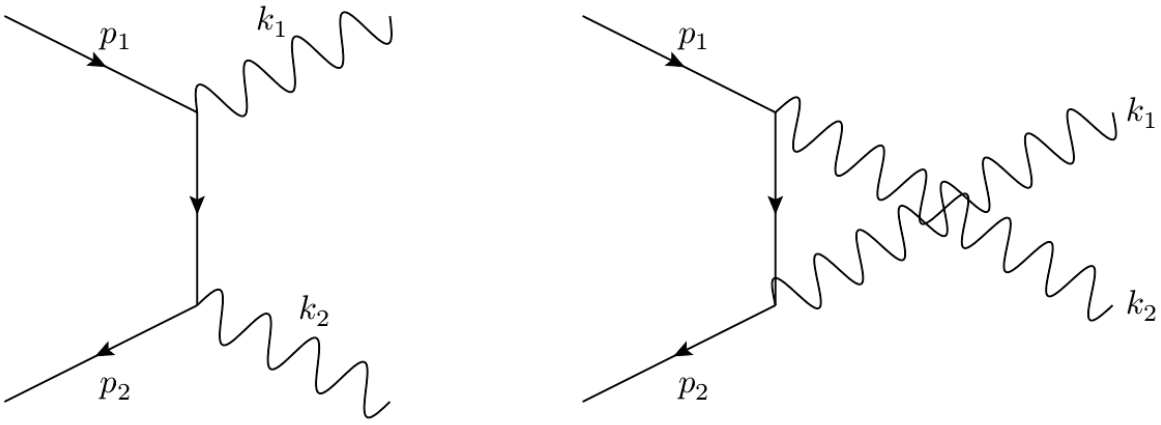

Figure 2.1: Feynman diagrams representing electron-positron pair annihilation to two photons, $e^+e^- \to \gamma\gamma$.

The amplitudes are,

$$\begin{aligned} \mathcal{M}_1 &= i\bar{v}(p_2)\left(ie\not{\epsilon}^\star(k_2)\right)\frac{i}{\not{p}_1 - \not{k}_1 - m}\left(ie\not{\epsilon}^\star(k_1)\right)u(p_1), \\ \mathcal{M}_2 &= i\bar{v}(p_2)\left(ie\not{\epsilon}^\star(k_1)\right)\frac{i}{\not{p}_1 - \not{k}_2 - m}\left(ie\not{\epsilon}^\star(k_2)\right)u(p_1), \end{aligned} \tag{2.1}$$

where u and v are the electron and positron spinors, respectively. The adjoint spinor $\bar{v} = v^\dagger\gamma^0$, and ϵ^μ is the polarization vector of a photon. p_i and k_i stand for incoming and outgoing momenta, respectively. We use the Feynman slash notation, $\not{p} = \gamma^\mu p_\mu$ where the Einstein summation is implied.

In the next step, $\mathcal{M}_1$ and $\mathcal{M}_2$ have to be evaluated. Since the p-Ps state is a spin singlet state, we have to substitute spinors with specific spins and perform the matrix multiplication in $\mathcal{M}_{1,2}$. However, the calculation gets tedious if we have more amplitudes in similar problems with specific spin condition. Therefore, a simple alternative, that can reduce the intricacy of the calculation, will be much desirable.

The amplitude is a product of two current terms that have gamma matrices sandwiched between a spinor and an adjoint spinor. We can rearrange the spinors in a current term as a matrix in the following way. Let s_1 and s_2 be two spinors, and they are connected with a matrix M in a current. The current term can be written as a trace,

$$\bar{s}_2 M s_1 = (\bar{s}_2)_i \, M_{ij} \, (s_1)_j = (s_1)_j \, (\bar{s}_2)_i \, M_{ij} = (s_1 \bar{s}_2)_{ji} \, M_{ij} = \mathrm{Tr}(s_1 \bar{s}_2 M). \tag{2.2}$$

The indices follow the Einstein summation. This implies $\mathcal{M}_{1,2}$ can be calculated as a multiplication of two traces. Eq. (2.2) is the key idea to calculate the amplitudes with preferred spin states. We know that any 4×4 matrices can be expressed in terms of gamma matrices. Therefore, we only need to find the gamma matrix representation of $s_1 \bar{s}_2$ for specific spins and use them to evaluate the amplitudes.

Electron and positron spinors are (first order approximation discarding momentum dependent terms $\mathcal{O}(\boldsymbol{p_i}^n)$)

$$u_\uparrow = \sqrt{2m} \begin{pmatrix} 1 \\ 0 \\ 0 \\ 0 \end{pmatrix}, u_\downarrow = \sqrt{2m} \begin{pmatrix} 0 \\ 1 \\ 0 \\ 0 \end{pmatrix}, v_\uparrow = \sqrt{2m} \begin{pmatrix} 0 \\ 0 \\ 0 \\ 1 \end{pmatrix}, v_\downarrow = \sqrt{2m} \begin{pmatrix} 0 \\ 0 \\ -1 \\ 0 \end{pmatrix}, \tag{2.3}$$

where m is the mass of electron (positron), and the subscript $\uparrow(\downarrow)$ specifies spin up (down). The matrix representation of all possible $s_1 \bar{s}_2$'s is given in table 2.1.

Table 2.1: $s_1 \bar{s}_2$-like spinor products in terms of gamma matrices (Dirac representation). u and v stand for electron and positron spinors, and their subscripts imply spin up ($\uparrow$) and down ($\downarrow$).

$s_1 \bar{s}_2$	gamma matrices presentation
$\frac{u_\uparrow \bar{u}_\uparrow}{2m}$	$\frac{1}{8}(1+\gamma^0)(\gamma^5+\gamma^3)(\gamma^5-\gamma^3)\gamma^0$
$\frac{u_\downarrow \bar{u}_\downarrow}{2m}$	$\frac{1}{8}(1+\gamma^0)(\gamma^5-\gamma^3)(\gamma^5+\gamma^3)\gamma^0$
$\frac{u_\uparrow \bar{u}_\downarrow}{2m}$	$-\frac{1}{4}(\gamma^5+\gamma^3)(\gamma^1+i\gamma^2)\gamma^0$
$\frac{u_\downarrow \bar{u}_\uparrow}{2m}$	$-\frac{1}{4}(\gamma^5-\gamma^3)(\gamma^1-i\gamma^2)\gamma^0$
$\frac{u_\uparrow \bar{v}_\uparrow}{2m}$	$\frac{1}{4}(1+\gamma^0)(\gamma^1+i\gamma^2)\gamma^0$
$\frac{u_\downarrow \bar{v}_\downarrow}{2m}$	$-\frac{1}{4}(1+\gamma^0)(\gamma^1-i\gamma^2)\gamma^0$
$\frac{u_\uparrow \bar{v}_\downarrow}{2m}$	$-\frac{1}{4}(1+\gamma^0)(\gamma^5+\gamma^3)\gamma^0$
$\frac{u_\downarrow \bar{v}_\uparrow}{2m}$	$\frac{1}{4}(1+\gamma^0)(\gamma^5-\gamma^3)\gamma^0$

The total amplitude, $\mathcal{M} = \mathcal{M}_1 + \mathcal{M}_2$ is computed using FORM [8]. The electron-positron pair forms a singlet state, $(\uparrow\downarrow - \downarrow\uparrow)/\sqrt{2}$. Transition amplitudes for $\uparrow\downarrow$ and $\downarrow\uparrow$ differ by a sign only,

$$\mathcal{M}_{\uparrow\downarrow} = -\mathcal{M}_{\downarrow\uparrow} = 2e^2 \tag{2.4}$$

where, e is the charge of the positron ($e > 0$). These amplitudes correspond to the emission of two right-handed photons. Therefore, the singlet amplitude for two right-handed photons is

$$\mathcal{M}(e^+e^- \to \gamma_R\gamma_R) = \frac{\mathcal{M}_{\uparrow\downarrow} - \mathcal{M}_{\downarrow\uparrow}}{\sqrt{2}} = 2\sqrt{2}e^2. \tag{2.5}$$

This is the amplitude when initial state is a pair of free electron and positron. If they form a bound state, the effective amplitude will be depend on the wave function, as we will see in the next subsection.

2.2.2 Bound State Amplitude

A bound state can be described as a superposition of free states with different momenta as it is shown in Eq. (5.43) in [9]. Then we can compute the bound state amplitude from the free state superposition of the bound state.

From [9], we can write,

$$|\text{p-Ps}\rangle = \sqrt{2M}\int \frac{d^3k}{(2\pi)^3}\tilde{\psi}(\boldsymbol{k})\frac{|\text{free } e^+e^-\rangle}{\sqrt{2m}\sqrt{2m}}, \tag{2.6}$$

where M is the mass of a Ps atom. $\sqrt{2m}$ in the denominator comes from the normalization of the spinors. The bound state amplitude is given by

$$\mathcal{M}(\text{p-Ps} \to \gamma_R\gamma_R) = \sqrt{2E}\int \frac{d^3k}{(2\pi)^3}\tilde{\psi}(\boldsymbol{k})\frac{\mathcal{M}(e^+e^- \to \gamma_R\gamma_R)}{\sqrt{2E_1}\sqrt{2E_2}} \tag{2.7}$$

where

$$\tilde{\psi}(\boldsymbol{k}) = \int d^3x\psi(\boldsymbol{x})e^{i\boldsymbol{k}.\boldsymbol{x}} \tag{2.8}$$

and $E_i = \sqrt{\boldsymbol{p}_i^2 + m^2}$, energy of the positron and electron. Since the particles in the atom are non-relativistic, we can drop $\mathcal{O}(\frac{\boldsymbol{p}_i^2}{m^2})$ terms and get $E_1 = E_2 \approx m$. We evaluate the amplitude in Eq. (2.7) and get

$$\mathcal{M}(\text{p-Ps} \to \gamma_R\gamma_R) = \frac{\sqrt{2M}}{2m}\mathcal{M}(e^+e^- \to \gamma_R\gamma_R)\int d^3x\psi(\boldsymbol{x})\int \frac{d^3k}{(2\pi)^3}e^{i\boldsymbol{k}.\boldsymbol{x}} \tag{2.9}$$

$$= \frac{\sqrt{2M}}{2m} \times 2\sqrt{2}e^2 \times \int d^3x\psi(\boldsymbol{x})\delta(\boldsymbol{x}) \tag{2.10}$$

$$= \frac{\sqrt{2M}}{m}\sqrt{2}e^2\psi(0), \tag{2.11}$$

where $\psi(0)$ is the value of the wave function at origin.

Eq. (2.11) tells us that when $\mathcal{O}(\frac{\boldsymbol{p}_i^2}{m^2})$ correction ignored, the bound state amplitude depends on $\psi(0)$, the probability of both particles meeting at the same point (i.e. the relative distance is zero).

2.2.3 Decay Rate

The decay rate is calculated integrating the probability density $|\mathcal{M}|^2$ over the outgoing momenta. We use Eq. (4.86) from [9],

$$\Gamma = \frac{1}{2M_A}\int d\Pi_{\text{LIPS}}\left|\mathcal{M}\left(M_A \to \{p_f\}\right)\right|^2 \tag{2.12}$$

to compute the decay rate of a bound state. M_A is the mass of bound state A that annihilates into other particles with momenta $\{p_f\}$ and

$$d\Pi_{\text{LIPS}} = (2\pi)^4\delta^4(p_A - \sum_f p_f)\prod_f \frac{d^3p_f}{(2\pi)^3}\frac{1}{2E_f}, \tag{2.13}$$

where LIPS stands for the Lorentz invariant phase space.

As we are looking into two-photon decay, we have implicitly specified this to be a system of Ps in singlet state, since only singlet states can decay into even number of photons. So the decay rate should be $\Gamma_{2\gamma} = \Gamma_{\text{p-Ps}\to 2\gamma}$ because there is no o-Ps present in the system of interest.

In this problem, $M_A = M$, mass of the Ps atom. Plugged in with the bound amplitude from Eq. (2.11), Eq. (2.12) gives the decay rate $\Gamma_{RR}(\text{p-Ps} \to \gamma_R\gamma_R)$ of p-Ps to emit two right-handed photons.

However, in $\int d\Pi_2$ integral, we sum over all momenta for the outgoing photons. Thus, photon states with momenta ($\boldsymbol{k}_1 = \boldsymbol{p}_{f,1}$,$\boldsymbol{k}_2 = \boldsymbol{p}_{f,2}$) and ($\boldsymbol{k}_1 = \boldsymbol{p}_{f,2}$,$\boldsymbol{k}_2 = \boldsymbol{p}_{f,1}$) are indistinguishable in the integral $\int \frac{d^3k_1}{2\omega_1}\frac{d^3k_2}{2\omega_2}$ (performed to derive Eq. (A.6)). Therefore, the phase space integral carries a double-counting of the same state, and a factor of $\frac{1}{2}$ is needed to

avoid the over-counting. In general, if there are N outgoing identical particles, we have to divide the appropriate version of Eq. (2.12) by $N!$ to remove the over-counting embedded in the phase space integral of $\int d\Pi_N$. $\frac{1}{N!}$ is the symmetry factor due to the outgoing identical particles, which is $\frac{1}{2}$ in our case. The decay rate expression becomes,

$$\Gamma_{RR} = \frac{1}{2} \times \frac{1}{2M} \int d\Pi_2 |\mathcal{M}(\text{p-Ps} \to \gamma_R \gamma_R)|^2 \tag{2.14}$$

$$= \frac{1}{2} \times \frac{1}{2M} \left(\frac{\sqrt{2M}}{m} \sqrt{2} e^2 \psi(0) \right)^2 \int d\Pi_2 \tag{2.15}$$

$$= \frac{1}{2} \times \frac{2e^4}{m^2} |\psi(0)|^2 \times \frac{1}{8\pi} \tag{2.16}$$

$$= \frac{2\pi\alpha^2}{m^2} |\psi(0)|^2 \quad (e^2 = 4\pi\alpha \text{ where } \hbar = c = \epsilon_0 = 1). \tag{2.17}$$

Adding contributions from both right-handed and left-handed photons, the total decay rate is $\Gamma = \Gamma_{RR} + \Gamma_{LL} = 2\Gamma_{RR} = \frac{4\pi\alpha^2}{m^2} |\psi(0)|^2$. The wave function solution in a hydrogen-like atom yields $|\psi_{1s}(0)|^2 = |\psi_{100}(0)|^2 = \frac{1}{\pi a^3}$, where Bohr radius $a_0 = \frac{4\pi\epsilon_0\hbar^2}{me^2} = \frac{1}{m\alpha}$. In a Ps atom, the effective mass $m_{\text{eff}} = \frac{m}{2}$; therefore, effective Bohr radius will be, $a = \frac{2}{m\alpha} (= 2a_0)$.

Therefore, $|\psi_{1s}(0)|^2 = \frac{m^3\alpha^3}{8\pi}$, and the final expression of $\Gamma = \frac{4\pi\alpha^2}{m^2} |\psi(0)|^2$ reduces to

$$\Gamma(\text{p-Ps} \to \gamma\gamma) = \frac{1}{2} m\alpha^5. \tag{2.18}$$

Eq. (2.18) is the p-Ps decay rate to the order of α^5 corroborating the experimental result [10]. We reproduced it employing the simple spinor matrix technique shown in Eq. (2.2) and using Table 2.1.

2.3 Single Photon Annihilation of Ps^-

In this section, we will study the single photon annihilation of Ps^-. First, we will write the 4-momenta of initial and final particles. Then we will calculate the amplitudes using the 4-momenta, the bound state amplitude, and the decay rate, respectively.

Ps^- consists of two electrons and a positron. The initial momenta are small compared to m, which determines the scale of transition amplitude. The ground state energy of Ps^- is also negligible compared to m. Therefore, we expand 4-momentum of any constituting particle in Ps^- with respect to $\frac{\boldsymbol{p}_i}{m}$ and obtain the first non-zero term, $(m, 0, 0, 0)$. We write $p_i = (m, 0, 0, 0)$, where $i = 1, 2, 3$ stand for the initial momenta of the electrons and the positron. We have two outgoing particles that must preserve 3-momentum; therefore, the decay products should have motion in the opposite direction to each other. We choose that

line to be z axis. Let the momenta of outgoing photon and electron be k_1 and k_2 such that $k_1 = (p, 0, 0, -p)$, $k_2 = (E, 0, 0, p)$. The conservation of 4-momentum and $k_2^2 = m^2$ provide

$$E + p = 3m, \tag{2.19}$$

$$E^2 - p^2 = m^2, \tag{2.20}$$

solving which we find $p = \frac{4}{3}m$ and $E = \frac{5}{3}m$. Thus $k_1 = (\frac{4}{3}m, 0, 0, -\frac{4}{3}m), k_2 = (\frac{5}{3}m, 0, 0, \frac{4}{3}m)$.

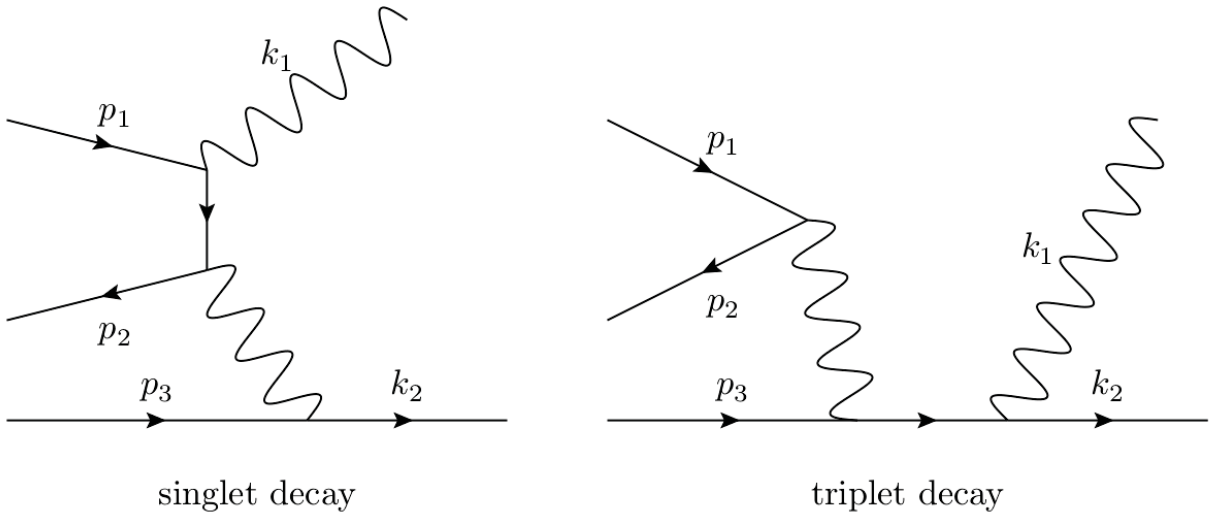

Figure 2.2: Feynman diagrams of $e^-e^+e^- \to e^-\gamma$ representing the annihilations of spin singlet and triplet e^+e^- pair in the Ps^- ion.

There are two ways Ps^- can emit a photon; the annihilating e^-e^+ pair can either convert into one or two photons, for a triplet or singlet pair, respectively. In the singlet decay, the remaining electron absorbs a virtual photon and the other photon goes out. In contrast, in the triplet decay, the remaining electron emits the outgoing photon absorbing the virtual photon from annihilation.

There are two possible e^-e^+ pairs for annihilation in each type of decay. The remaining electron can absorb any one of the two photons in the singlet case; similarly the order of absorption and emission in the triplet decay provides two possibilities. Therefore, we will have 4 diagrams in each of the singlet and triplet decays; the two representative diagrams are shown in Fig. 2.2 out of 8 diagrams. Their amplitudes are computed in the following subsection.

2.3.1 Amplitudes

We will denote the spin assignment of $e^-e^+e^- \to e^-\gamma$ following the order of the particles as written here. For example, the up-down arrows in $\uparrow\uparrow\downarrow\to\downarrow\uparrow$ imply the spins as (1st) electron up, (2nd) positron up, and (3rd) electron down on the left-hand side and (outgoing) electron up and photon down on the right-hand side, respectively.

Let's consider the case where the positron spin is up. Since the electron pair will form a singlet state in the ground state ($\ell = 0$) of Ps^- ion, the total angular momentum is determined by the positron spin, which is $+1/2$. Only if the photon spin is $+1$ and the outgoing electron spin is $-1/2$, then angular momentum is conserved ($+1/2 = +1 - 1/2$). In the definition of k_1, the photon is going in the $-z$ direction. Therefore, it must be a left-handed photon, i.e. spin $+1$ with motion in the opposite direction of the spin. If the positron state is spin down, the outgoing photon will be right-handed. Because of parity conservation, the probabilities of left and right handed photon emission must be equal. Therefore, we choose to calculate only the left-handed photon case i.e. for positron spin up.

The general expression for the singlet and triplet decay amplitudes are

$$\mathcal{M}_S = \frac{1}{(k_2-p_3)^2}\left(\bar{v}(p_2)\,(ie\gamma_\mu)\,\frac{i}{\not{p}_1 - \not{k}_1 - m}\,(ie\not{\epsilon}^\star(k_1))\,u(p_1)\right)\left(\bar{u}(k_2)\,(ie\gamma^\mu)\,u(p_3)\right), \quad (2.21)$$

$$\mathcal{M}_T = \frac{1}{(p_1+p_2)^2}\left(\bar{v}(p_2)\,(ie\gamma_\mu)\,u(p_1)\right)\left(\bar{u}(k_2)\,(ie\not{\epsilon}^\star(k_1))\,\frac{i}{\not{k}_2 - \not{k}_1 - m}\,(ie\gamma^\mu)\,u(p_3)\right). \quad (2.22)$$

The contributions of all the diagrams will be generated with the careful interchange of labels such as $1 \leftrightarrow 3$, appropriate virtual momentum, and the correct ordering of the matrices for a corresponding diagram. Eq. (2.2) will be helpful again to convert the matrix multiplication in the amplitudes to a trace calculation. The spinor for the free outgoing electron can be expressed in terms of the basis spinors in Eq. (2.3),

$$U_\uparrow = \sqrt{E+m}\begin{pmatrix}1\\0\\\frac{p_z}{E+m}\\0\end{pmatrix} = \sqrt{\frac{8m}{3}}\begin{pmatrix}1\\0\\\frac{1}{2}\\0\end{pmatrix} = \sqrt{\frac{8m}{3}}\left(\frac{u_\uparrow - \frac{1}{2}v_\downarrow}{\sqrt{2m}}\right) = \sqrt{\frac{4}{3}}\left(u_\uparrow - \frac{1}{2}v_\downarrow\right) \quad (2.23)$$

$$U_\downarrow = \sqrt{E+m}\begin{pmatrix}0\\1\\0\\-\frac{p_z}{E+m}\end{pmatrix} = \sqrt{\frac{8m}{3}}\begin{pmatrix}0\\1\\0\\-\frac{1}{2}\end{pmatrix} = \sqrt{\frac{8m}{3}}\left(\frac{u_\downarrow - \frac{1}{2}v_\uparrow}{\sqrt{2m}}\right) = \sqrt{\frac{4}{3}}\left(u_\downarrow - \frac{1}{2}v_\uparrow\right) \quad (2.24)$$

substituting $p_z = \frac{4}{3}m, E = \frac{5}{3}m$. We can check the normalization of U as $U^\dagger U = 2E$. Eq. (2.24) will be used as the spinor of outgoing electron in this problem, where the positron spin is strictly up. We rearranged the expression of $\mathcal{M}_S$ and $\mathcal{M}_T$ following the "spinor matrix" construction in Eq. (2.2) and putting the spinor matrices from Table 2.1. A program in FORM produced the trace values and the amplitudes. We list all the amplitudes for positron up in table 2.2.

Table 2.2: Amplitude values $\mathcal{M}$ for the 8 Feynman diagrams of $\mathrm{Ps}^- \to e^-\gamma$ when the positron spin is up.

$\times\frac{1}{\sqrt{6}}\frac{ie^3}{m}$	$\mathcal{M}_{\uparrow\uparrow\downarrow\to\downarrow\uparrow}$	$\mathcal{M}_{\downarrow\uparrow\uparrow\to\downarrow\uparrow}$
$\mathcal{M}_1$	-2	$+1$
$\mathcal{M}_2$	0	-1
$\mathcal{M}_3$	-1	$+2$
$\mathcal{M}_4$	$+1$	0
$\mathcal{M}_5$	-9	0
$\mathcal{M}_6$	$+9$	-6
$\mathcal{M}_7$	0	$+9$
$\mathcal{M}_8$	$+6$	-9
$\sum\mathcal{M}_i$	$\mathcal{M}_{\uparrow\cdot\downarrow} = 4$	$\mathcal{M}_{\downarrow\cdot\uparrow} = -4$

Since the electron pair forms a singlet, we write the sum of the amplitudes in singlet superposition and find

$$\mathcal{M} = \frac{\mathcal{M}_{\uparrow\cdot\downarrow} - \mathcal{M}_{\downarrow\cdot\uparrow}}{\sqrt{2}} = \frac{+4-(-4)}{\sqrt{2}}\sqrt{\frac{1}{6}}\frac{ie^3}{m} = 4\sqrt{\frac{1}{3}}\frac{ie^3}{m} \tag{2.25}$$

giving

$$|\mathcal{M}|^2 = \frac{16}{3}\frac{e^6}{m^2}. \tag{2.26}$$

Eq. (2.26) provides the leading order amplitude when all three initial particles (e^-, e^+, e^-) are free.

2.3.2 Bound State Amplitude

Similarly to the expression of p-Ps bound state in Eq. (2.6), we can write

$$|\mathrm{Ps}^-\rangle = \sqrt{2M}\int \frac{d^3k_1}{(2\pi)^3}\frac{d^3k_2}{(2\pi)^3}\tilde{\psi}(\boldsymbol{k_1},\boldsymbol{k_2})\frac{|\text{free } e^-e^+e^-\rangle}{\sqrt{2m}\sqrt{2m}\sqrt{2m}}, \tag{2.27}$$

where, $\tilde{\psi}(\boldsymbol{k_1}, \boldsymbol{k_2})$ and M are the momentum-space wave function and the mass of Ps^-.

$$\mathcal{M}(\mathrm{Ps}^- \to e^-\gamma) = \sqrt{2M}\int \frac{d^3k_1}{(2\pi)^3}\frac{d^3k_2}{(2\pi)^3}\tilde{\psi}(\boldsymbol{k_1}, \boldsymbol{k_2})\frac{\mathcal{M}(e^-e^+e^- \to e^-\gamma)}{\sqrt{2m}\sqrt{2m}\sqrt{2m}} \tag{2.28}$$

$$= \sqrt{\frac{2M}{(2m)^3}}\mathcal{M}(e^-e^+e^- \to e^-\gamma)$$

$$\times \int d^3x_1 d^3x_2 \psi(\boldsymbol{x_1}, \boldsymbol{x_2}) \int \frac{d^3k_1}{(2\pi)^3}\frac{d^3k_2}{(2\pi)^3} e^{i\boldsymbol{k_1}.\boldsymbol{x_1}} e^{i\boldsymbol{k_2}.\boldsymbol{x_2}} \tag{2.29}$$

$$= \sqrt{\frac{2M}{(2m)^3}}\mathcal{M}(e^-e^+e^- \to e^-\gamma)\psi(0,0) \tag{2.30}$$

2.3.3 Decay Rate

Since we have two identical electrons, we have to include $\frac{1}{2}$ prefactor in the expression of the decay rate. This prefactor arises from the operator algebra and the normalization of the bound state, explained in Appendix B.2. We again use Eq. (2.12),

$$\Gamma(\mathrm{Ps}^- \to e^-\gamma) = \frac{1}{2} \times \frac{1}{2M}\int d\Pi_2 |\mathcal{M}(\mathrm{Ps}^- \to e^-\gamma)|^2 \tag{2.31}$$

$\int d\Pi_2 = \frac{1}{9\pi}$ from Eq. (A.17). Using Eq. (2.26), we obtain the decay rate of Ps^-, when the positron spin is up (emitting a left-handed photon).

$$\Gamma(\mathrm{Ps}^- \to e^-\gamma_L) = \frac{1}{2} \times \frac{1}{2M} \times \left(\sqrt{\frac{2M}{(2m)^3}}\mathcal{M}(e^-e^+e^- \to e^-\gamma_L)\psi(0,0)\right)^2 \int d\Pi_2 \tag{2.32}$$

$$= \frac{1}{2} \times \frac{1}{2M} \times \frac{2M}{(2m)^3}\frac{16}{3}\frac{e^6}{m^2}|\psi(0,0)|^2 \times \frac{1}{9\pi} \quad \text{(From Eq.(2.26))} \tag{2.33}$$

$$= \frac{64\pi^2\alpha^3}{27m^5}|\psi(0,0)|^2. \tag{2.34}$$

The decay rate for positron spin down (a right-handed photon) will be same as Eq. (2.34). Therefore, the total decay rate will be average of the initial states (in this case, positron state), giving

$$\Gamma(\mathrm{Ps}^- \to e^-\gamma) = \frac{\Gamma_{\text{positron up}} + \Gamma_{\text{positron down}}}{2} = \frac{64\pi^2\alpha^3}{27m^5}|\psi(0,0)|^2. \tag{2.35}$$

Eq. (2.35) confirms Kryuchkov's result in [4].

2.4 Conclusion

In this chapter, we reproduced the decay rates of p-Ps and Ps^- using the spinor matrix technique described in 2.2.1. This reduces the toll of calculations and yields results with fewer terms. For example, in [4], Kryuchkov summed eight amplitudes $\mathcal{M}$, converted the square $|\mathcal{M}|^2$ to a trace, and computed the final result in Mathematica. In the final step, the program had to execute the expression $|\mathcal{M}|^2$ containing 64 terms. In contrast, we derived Eq. (2.35) considering 8 amplitude terms. If we wished, it is also possible to complete the trace calculation by hand instead of any computational tool. This demonstrates the level of simplicity we accomplished with this method.

Chapter 3

Decay Rate of Di-positronium Molecule

3.1 Introduction

Ps_2 is a hydrogen-like molecule consisting of two Ps atoms. Wheeler predicted its existence in his 1946 paper on polyelectrons [11]. Ps has a short lifetime, and it is cumbersome to produce a large number of low-energy positrons. Therefore, it took more than six decades to find it in a laboratory [7]. This is the first matter-antimatter molecule produced in an experiment.

In the meantime, this molecule has been extensively studied theoretically. Decay rates of possible Ps_2 decay channels have been computed numerically [12]. The analytical calculation of two-photon total annihilation of Ps_2 is shown in [13], where the authors did not consider all Feynman diagrams corresponding to the leading order. There are 40 diagrams but only 8 of them were calculated in [13].

In this section, we have performed the full calculation for the ground state of Ps_2 by taking into account of all 40 diagrams. We will use the approach constructed in Chapter 2, and derive the decay rate analytically.

3.2 Two-photon Total Annihilation of Ps_2

In this section, we will define the symbols and classify the diagrams for $Ps_2 \to \gamma\gamma$ channel. Then we will calculate amplitudes, bound state amplitudes, and the decay rate.

We consider the following notation

$$e^-(p_1) + e^+(p_2) + e^-(p_3) + e^+(p_4) \to \gamma(k_1) + \gamma(k_2),$$

to denote the momenta of the constituting particles in Ps_2 and the outgoing photons. Similar

to the calculation for Ps^-, we keep the leading order term in the incoming momenta i.e. $p_i = (m, 0, 0, 0)$, where i goes from 1 to 4 for the incoming particles, and therefore, $k_1 = (2m, 0, 0, 2m)$ and $k_2 = (2m, 0, 0, -2m)$ preserving 4-momentum.

The leading-order diagrams of $Ps_2 \to \gamma\gamma$ have 4 vertices. We have categorized them into three classes- namely A, B, and C shown in Fig. 3.1. Each e^+e^- pair emits a photon in class A diagrams, where one pair emits both photons in class B diagrams. The class C is similar to B, but the virtual photon from one e^+e^- pair is absorbed by the virtual electron, whereas it is absorbed by a real particle (e^- or e^+) in B.

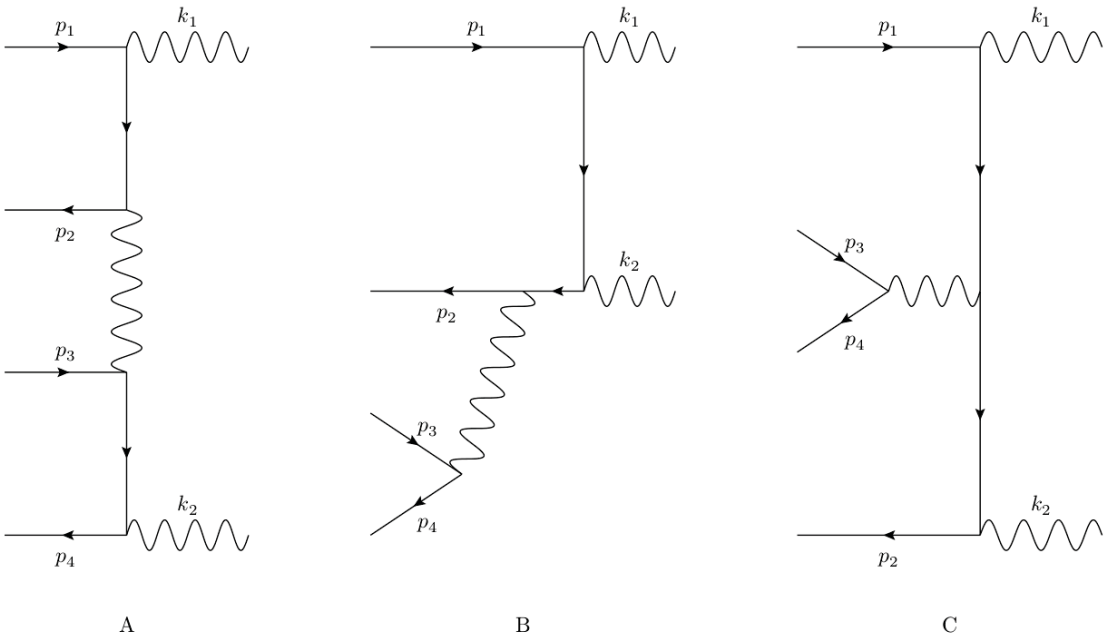

Figure 3.1: Three classes of diagrams corresponding to $Ps_2 \to \gamma\gamma$.

There are 16 diagrams in class A. We can arrange the initial identical particles in three possible ways to generate this class of diagrams. These are interchanging between (i) e^- pair, (ii) e^+ and e^- in each of the pairs, and (iii) outgoing photon pair. There are 2 ways to draw the positions of e^+ and e^- in a pair; for two pairs of e^+e^- there will be 4 ways. Interchanging between e^- pair and photon pair will create 2 and 2 ways of drawing diagrams, respectively. Altogether we get $2^4 = 16$ diagrams in class A.

In class B, we can interchange between (i) e^- pair, (ii) e^+ and e^- in the pair that emits real photons, (iii) e^+e^- pairs between them such as $12 \rightleftarrows 34$, and (iv) outgoing photon pair. This contributes another $2^4 = 16$ diagrams. Similarly, class C will accommodate $2^3 = 8$ diagrams crossing (i) e^- pair, (ii) both e^+e^- pairs and (iii) outgoing photon pair.

In total, we have 16+16+8=40 diagrams from these three classes.

3.2.1 Amplitudes

As we have identified all the diagram classes for the decay, now we will write the general expressions of amplitudes for A,B, and C.

Amplitudes for the representative diagrams shown in Fig. 3.1 are

$$\mathcal{M}_A = \frac{1}{(p_1+p_2-k_1)^2}\left(\bar{v}(p_2)\gamma_\mu \frac{i}{\not{p}_1 - \not{k}_1 - m}\not{\epsilon}^\star(k_1)u(p_1)\right)\left(\bar{v}(p_4)\not{\epsilon}^\star(k_2)\frac{i}{\not{k}_2 - \not{p}_4 - m}\gamma^\mu u(p_3)\right), \tag{3.1}$$

$$\mathcal{M}_B = \frac{1}{(p_3+p_4)^2}\left(\bar{v}(p_2)\gamma_\mu \frac{i}{\not{p}_1 - \not{k}_1 - \not{k}_2 - m}\not{\epsilon}^\star(k_2)\frac{i}{\not{p}_1 - \not{k}_1 - m}\not{\epsilon}^\star(k_1)u(p_1)\right)\left(\bar{v}(p_4)\gamma^\mu u(p_3)\right), \tag{3.2}$$

$$\mathcal{M}_C = \frac{1}{(p_3+p_4)^2}\left(\bar{v}(p_2)\not{\epsilon}^\star(k_2)\frac{i}{\not{k}_2 - \not{p}_4 - m}\gamma_\mu \frac{i}{\not{p}_1 - \not{k}_1 - m}\not{\epsilon}^\star(k_1)u(p_1)\right)\left(\bar{v}(p_4)\gamma^\mu u(p_3)\right). \tag{3.3}$$

All the other 37 amplitudes are generated switching momenta in these expressions.

We used the spinor matrices in Table 2.1 along with the technique in Eq. (2.2) to compute the amplitude $\mathcal{M}$'s for emitting two right-handed photons for these particular spin combinations using FORM and summed for all 40 diagrams. We would like to put a remark about the relation among these $\mathcal{M}'$s for specific spin combinations. Since we were computing the amplitudes one by one for specific spins, we could verify a simple crossing symmetry of the identical particles. For an example, if electrons are crossed for two diagrams (say $\mathcal{M}_i$ and $\mathcal{M}_j$), $\mathcal{M}_i(\uparrow\uparrow\downarrow\downarrow) = \mathcal{M}_j(\downarrow\uparrow\uparrow\downarrow)$. In other words, different diagrams will yield the same value of amplitudes for different spin configurations. Tracing $\mathcal{M}$ value from this symmetry can sometimes reduce the toll of computing all diagrams when we have specific spin preferences. It is also an efficient and simple way to check the results.

We consider the ground state of Ps_2, i.e., both electron and positron pairs are in the singlet state. Spin notation with arrows will be denoted such that 1st and 3rd spins are electrons, and 2nd and 4th spins are positrons.

$$|S=0, m_s=0\rangle_{\mathrm{Ps}_2} = |0,0\rangle_{e^-\text{ pair}} \otimes |0,0\rangle_{e^+\text{ pair}} \tag{3.4}$$

$$= \frac{(\uparrow\downarrow - \downarrow\uparrow)}{\sqrt{2}} \cdot \frac{(\uparrow\downarrow - \downarrow\uparrow)}{\sqrt{2}} \tag{3.5}$$

$$= \frac{1}{2}\left(\uparrow\uparrow\downarrow\downarrow - \uparrow\downarrow\downarrow\uparrow - \downarrow\uparrow\uparrow\downarrow + \downarrow\downarrow\uparrow\uparrow\right) \tag{3.6}$$

The ground state can only emit photon pair that will preserve the total angular momentum, which implies outgoing photons must be both either right-handed or left-handed. C diagram

Table 3.1: Amplitude values for A (left) and B class diagrams in $Ps_2 \to \gamma\gamma$ decay.

$\times\frac{ie^4}{m^2}$	$\uparrow\uparrow\downarrow\downarrow$	$\uparrow\downarrow\downarrow\uparrow$	$\downarrow\uparrow\uparrow\downarrow$	$\downarrow\downarrow\uparrow\uparrow$
$\mathcal{M}_1$	-1	0	0	0
$\mathcal{M}_2$	$+1$	-1	0	0
$\mathcal{M}_3$	$+1$	0	-1	0
$\mathcal{M}_4$	0	0	0	-1
$\mathcal{M}_5$	0	0	$+1$	0
$\mathcal{M}_6$	-1	0	0	0
$\mathcal{M}_7$	0	0	-1	$+1$
$\mathcal{M}_8$	0	0	-1	$+1$
$\mathcal{M}_9$	0	-1	0	$+1$
$\mathcal{M}_{10}$	$+1$	0	-1	0
$\mathcal{M}_{11}$	0	$+1$	0	0
$\mathcal{M}_{12}$	0	0	0	-1
$\mathcal{M}_{13}$	0	0	$+1$	0
$\mathcal{M}_{14}$	$+1$	-1	0	0
$\mathcal{M}_{15}$	0	-1	0	$+1$
$\mathcal{M}_{16}$	0	$+1$	0	0
$\mathcal{M}_{tot,A}$	$+2$	-2	-2	$+2$

$\times\frac{ie^4}{m^2}$	$\uparrow\uparrow\downarrow\downarrow$	$\uparrow\downarrow\downarrow\uparrow$	$\downarrow\uparrow\uparrow\downarrow$	$\downarrow\downarrow\uparrow\uparrow$
$\mathcal{M}_1$	$-1/2$	0	$+1/4$	0
$\mathcal{M}_2$	0	$+1/4$	0	$-1/2$
$\mathcal{M}_3$	$-1/2$	$+1/4$	0	0
$\mathcal{M}_4$	0	0	$+1/4$	$-1/2$
$\mathcal{M}_5$	$-1/2$	$+1/4$	0	0
$\mathcal{M}_6$	0	0	$+1/4$	$-1/2$
$\mathcal{M}_7$	0	$+1/4$	0	$-1/2$
$\mathcal{M}_8$	$-1/2$	0	$+1/4$	0
$\mathcal{M}_9$	0	0	$+1/2$	$-1/4$
$\mathcal{M}_{10}$	$-1/4$	$+1/2$	0	0
$\mathcal{M}_{11}$	0	$+1/2$	0	$-1/4$
$\mathcal{M}_{12}$	$-1/4$	0	$+1/2$	0
$\mathcal{M}_{13}$	0	$+1/2$	0	$-1/4$
$\mathcal{M}_{14}$	$-1/4$	0	$+1/2$	0
$\mathcal{M}_{15}$	0	0	$+1/2$	$-1/4$
$\mathcal{M}_{16}$	$-1/4$	$+1/2$	0	0
$\mathcal{M}_{tot,B}$	-3	$+3$	$+3$	-3

contribution is zero i.e. $\mathcal{M}_{tot,C} = 0$. $\mathcal{M} = \mathcal{M}_{tot,A} + \mathcal{M}_{tot,B} + \mathcal{M}_{tot,C}$ yields,

$$\left.\begin{aligned} \mathcal{M}_{\uparrow\uparrow\downarrow\downarrow} &= -1 \\ \mathcal{M}_{\uparrow\downarrow\downarrow\uparrow} &= +1 \\ \mathcal{M}_{\downarrow\uparrow\uparrow\downarrow} &= +1 \\ \mathcal{M}_{\downarrow\downarrow\uparrow\uparrow} &= -1 \end{aligned}\right\} \times \frac{ie^4}{m^2}. \tag{3.7}$$

From Eq. (3.6) and (3.7),

$$\mathcal{M}(e^+e^-e^+e^- \to \gamma_R\gamma_R) = \frac{1}{2}\sum_{\text{40 diagrams}} \left(\mathcal{M}_{\uparrow\uparrow\downarrow\downarrow} - \mathcal{M}_{\uparrow\downarrow\downarrow\uparrow} - \mathcal{M}_{\downarrow\uparrow\uparrow\downarrow} + \mathcal{M}_{\downarrow\downarrow\uparrow\uparrow}\right) \tag{3.8}$$

$$= -\frac{2ie^4}{m^2}. \tag{3.9}$$

This free state amplitude is the contribution of all diagrams for emitting two right-handed

photons. We will use this result to find the bound state amplitude of Ps_2 in Eq. (3.13).

3.2.2 Bound State Amplitude

We construct the bound state amplitude connecting the bound state wave function and the free state amplitude in Eq. (3.9). There are 12 coordinate variables for 4-particles wave function. We assume the center of mass to be fixed which reduces the number of required coordinates to 9 that will be denoted by $\{\boldsymbol{x_1}, \boldsymbol{x_2}, \boldsymbol{x_3}\}$, defined as the separation vectors between the initial particles. Fourier transform of the ground state wave function $\psi(\boldsymbol{x_1}, \boldsymbol{x_2}, \boldsymbol{x_3})$ provides the momentum space wave function, $\tilde{\psi}(\boldsymbol{k_1}, \boldsymbol{k_2}, \boldsymbol{k_3})$. We expand the bound state as a superposition of free electron and positron states in momentum space (as already shown in Chapter 2),

$$|\mathrm{Ps}_2\rangle = \sqrt{2M} \int \frac{d^3k_1}{(2\pi)^3} \frac{d^3k_2}{(2\pi)^3} \frac{d^3k_3}{(2\pi)^3} \tilde{\psi}(\boldsymbol{k_1}, \boldsymbol{k_2}, \boldsymbol{k_3}) \frac{|\text{free } e^+e^-e^+e^-\rangle}{\sqrt{2m}\sqrt{2m}\sqrt{2m}\sqrt{2m}}, \tag{3.10}$$

where M is the mass of the Ps_2, and $\tilde{\psi}(\boldsymbol{k_1}, \boldsymbol{k_2}, \boldsymbol{k_3})$ is the free particle wave function in momentum space. It yields

$$\mathcal{M}(\mathrm{Ps}_2 \to \gamma_R\gamma_R) = \sqrt{\frac{2M}{(2m)^4}} \int \frac{d^3k_1}{(2\pi)^3} \frac{d^3k_2}{(2\pi)^3} \frac{d^3k_3}{(2\pi)^3} \tilde{\psi}(\boldsymbol{k_1}, \boldsymbol{k_2}, \boldsymbol{k_3}) \mathcal{M}(e^+e^-e^+e^- \to \gamma_R\gamma_R) \tag{3.11}$$

$$= \sqrt{\frac{2M}{(2m)^4}} \mathcal{M}(e^+e^-e^+e^- \to \gamma_R\gamma_R) \int d^3x_1 d^3x_2 d^3x_3 \psi(\boldsymbol{x_1}, \boldsymbol{x_2}, \boldsymbol{x_3})$$

$$\times \int \frac{d^3k_1}{(2\pi)^3} \frac{d^3k_2}{(2\pi)^3} \frac{d^3k_3}{(2\pi)^3} e^{i\boldsymbol{k_1}.\boldsymbol{x_1}} e^{i\boldsymbol{k_2}.\boldsymbol{x_2}} e^{i\boldsymbol{k_3}.\boldsymbol{x_3}} \tag{3.12}$$

$$= \sqrt{\frac{2M}{(2m)^4}} \left(-\frac{2ie^4}{m^2}\right) \psi(0,0,0). \tag{3.13}$$

The decay rate ($\sim |\mathcal{M}|^2$) will be eventually proportional to $|\psi(0,0,0)|^2$, an intuitive requirement for all the particles to annihilate at one point and produce photons.

3.2.3 Decay Rate

We will use the master formula Eq. (2.12) to evaluate the decay rate. We will have a factor of $\frac{1}{2^3}$ for the participating identical particles (e^-, e^+, γ) and $\frac{1}{2^4}$ to count the contribution for

the singlet state only out of 2^4 distinct spin states. We have,

$$\Gamma_{RR} = \Gamma(\mathrm{Ps}_2 \to \gamma_R\gamma_R) = \frac{1}{2^4} \times \frac{1}{2^3} \times \frac{1}{2M} \int d\Pi_2 \left|\mathcal{M}(\mathrm{Ps}_2 \to \gamma_R\gamma_R)\right|^2 \tag{3.14}$$

$$= \frac{1}{2^7} \times \frac{1}{2M} \left| \sqrt{\frac{2M}{(2m)^4}} \left(-\frac{2ie^4}{m^2}\right) \psi(0,0,0) \right|^2 \int d\Pi_2 \tag{3.15}$$

$$= \frac{1}{2^9 m^4} \left(\frac{(4\pi\alpha)^4}{m^4}\right) |\psi(0,0,0)|^2 \times \frac{1}{8\pi} \tag{3.16}$$

$$= \frac{\pi^3\alpha^4}{16m^8} \left|\psi(0,0,0)\right|^2. \tag{3.17}$$

where, $\int d\Pi_2 = \dfrac{1}{8\pi}$, for two outgoing photons from Eq. (A.6) derived later. The rate should be same for emitting left-handed photons as well.

Therefore, the total rate,

$$\Gamma(\mathrm{Ps}_2 \to \gamma\gamma) = \Gamma_{RR} + \Gamma_{LL} = 2\Gamma_{RR} = \frac{\pi^3\alpha^4}{8m^8} \left|\psi(0,0,0)\right|^2 \tag{3.18}$$

where $\left|\psi(0,0,0)\right|^2 = 4.5 \times 10^{-6} a_0^{-9}$ (as employed in [13], a_0 = the Bohr radius). Inserting the relation between SI and natural units, we find $\Gamma(\mathrm{Ps}_2 \to \gamma\gamma) = 2.25 \times 10^{-12} s^{-1}$.

Eq. (3.18) is the main result of this chapter. After carefully considering all 40 diagrams, we find our result to be 4.07 times smaller than the previous result with 8 diagrams [13].

3.3 Conclusion

Aside from the remarkable success of being the first matter-antimatter molecule, the production of Ps_2 has a promising future to create high intensity laser beam [14]. With its decay, Ps_2 produces spin-polarized Ps atoms, and if cooled enough, those Ps atoms can form a Bose-Einstein condensate. The condensate may produce coherent gamma rays when annihilated, generating a laser beam more powerful than current laser technology. However, attaining the milestone may not be possible in the near future for experimental challenges.

Our purpose for this calculation was to apply the theoretical tools constructed in Chapter 2 and complement the existing theoretical analysis of the description of Ps_2. We provide the correct decay rate for two-photon total annihilation of Ps_2, which will be published soon. Most importantly, we learned how to compute a bound state decay rate with minimum intricacy. Similarly, we can investigate the decay nature of other short-lived compounds with a positron i.e., PsH.

Chapter 4

Search for Muon to Electron Conversion

4.1 Introduction

In the Standard Model (SM), there are three flavors of leptons. Each lepton flavor is approximately conserved, up to effects suppressed by neutrino masses. Lepton numbers are conserved individually and as a total in any interaction. However, the neutrino oscillation refutes the basis of the conservation of the lepton number.

Charged leptons have mass eigenstates as the Hamiltonian eigenstates unlike the neutrinos; therefore, it is not feasible to observe oscillation among electron, muon, and tau lepton. Nevertheless, the neutrino oscillation can cause the charged lepton flavor violation (CLFV), which is depicted in diagram A in Fig. (4.1). The neutrino in the interaction changes its flavor, and the W boson becomes a new charged lepton absorbing the "new" neutrino after emitting a photon. On the other hand, theories Beyond the Standard Model (BSM) can accommodate the CLFV independently with new type of interactions.

In this chapter, we will discuss possible CLFV processes in BSM and experimental searches for it ($\mu - e$ conversion), and we will state the problem of bound muon decay which arose as a background in the conversion search.

4.2 BSM Processes for CLFV and Experimental Endeavor

The search for $\mu \to e\gamma$ dates back to 1947 [15] before the discovery of neutrino. In that work, Hincks and Pontecorvo set an upper limit on the branching ratio of less than 10% for this decay channel. The upper limit improved with more experiments conducted later, and motivation for the CLFV search has gradually centered around BSM theories.

Muon is the optimal particle for CLFV process, because of its long lifetime and copious production, thanks to its light mass in comparison with tau lepton. Its lifetime allows it to

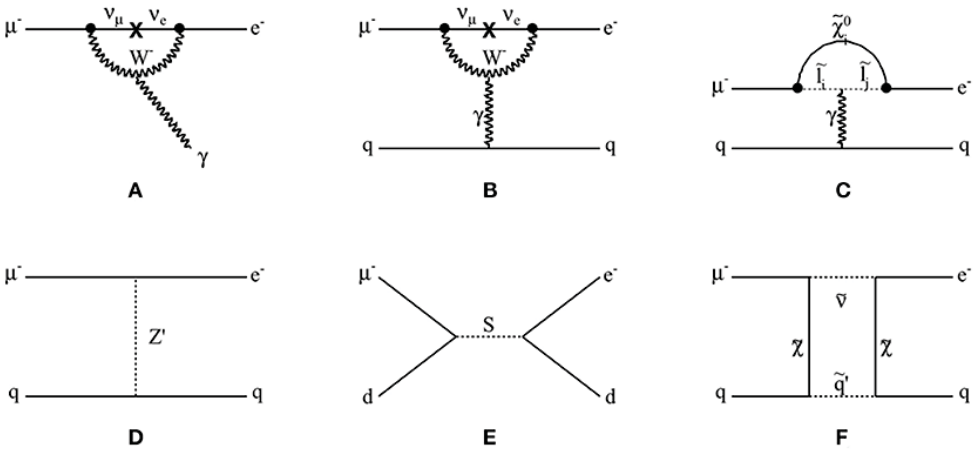

Figure 4.1: Diagrams corresponding to the $\mu - e$ conversion, (A) for $\mu^+ \to e^+ + \gamma$, (B-F) for $\mu^- + N \to e^- + N$. (A-B) describes SM processes due to massive neutrino, (C) is a supersymmetric (SUSY) process in a loop diagram, (D) and (E) are vector boson and scalar boson exchanges processes, and (F) is another SUSY process in a box diagram. [1]

stay longer in the atomic orbit before it disintegrates into an electron. For example of the efficiency of production, only $1 \sim 10$ tau lepton pair productions per second were found in the B-factory data, while the future muon conversion experiments will generate $10^{13} \sim 10^{14}$ muons per second. Therefore, the huge flux of muons will make the search for $\mu - e$ conversion possible.

There are three types of CLFV processes important in the experiments $\mu^- + N \to e^- + N$, $\mu^+ \to e^+ + \gamma$, and $\mu^+ \to e^+ e^- e^+$. In the first process, muon converts into electron while bound in an atom. A diagram with radiationless conversion is shown in diagram B, where the virtual photon interacts with the nucleus. There can be hypothetical interactions shown in diagrams C-F where conversion occurs without involving any neutrino. These are the proposed BSM interactions. There can be a charged supersymmetric particle with photon interaction to quarks, as shown in diagram C as well as direct lepton-quark interaction depicted in D-F. The effective Lagrangian of $\mu - e$ conversion process is

$$\begin{aligned} \mathcal{L}_{CLFV} = & \frac{1}{(1+\kappa)\Lambda^2} m_\mu \bar{\mu}_R \sigma^{\mu\nu} e_L F_{\mu\nu} \\ & + \frac{\kappa}{(1+\kappa)\Lambda^2} \left(\bar{\mu}_L \gamma^\mu e_L\right) \left(\bar{u}_L \gamma_\mu u_L + \bar{d}_L \gamma_\mu d_L\right) + \text{H.C.}, \end{aligned} \tag{4.1}$$

where the first term stands for $\mu \to e + \gamma$ and the second term gives contact interaction of two leptons and two quarks. μ, e, d, u are fields of the interacting particles [16]. We have two free parameters Λ and κ that describe the energy scale of the CLFV process and the relative strength of the two terms respectively.

Since SM process involves neutrino oscillations, its contribution is negligible, because the rate of neutrino oscillation is extremely small for the tiny mass of neutrino, and the heavy mass of W boson suppresses the SM interaction in the denominator. Therefore, BSM theories predict a higher rate of CLFV compared to the unobservable branching ratios of about 10^{-54} estimated by the SM [17]. Consequently, any observation of the CLFV process can be a direct signature of BSM theories.

Mu2e experiment in Fermilab differs from previous $\mu - e$ conversion experiments in three major ways: using a novel solenoid system for the formation of the muon beam, producing 10000 times stronger intensity of the muon beam than earlier experiments, and generating a pulsed beam with a long time gap between pulses to reduce backgrounds [2]. The background events arise from the pion decays or other beam particles. The pulsed muon beam ensures to discard these beam related backgrounds out of the muon capture events. The experiment will begin its operations in 2022, taking data for 3 years. It will examine $\sim 10^{18}$ stopped muons with a single event sensitivity of 3×10^{-17}.

The COMET experiment in J-PARC, Japan has similarity with Mu2e in operational aspects such as pulsed muon beam, level of sensitivity, and aluminum target. COMET has two phases; Phase-I experiment has an estimated single event sensitivity of 3×10^{-15}. The COMET Phase-II will achieve $\mathcal{O}(10^{-17})$ conversion sensitivity.

It is hard to predict that the conversion can be found even within the extraordinary sensitivity achieved in these experiments. Provided any trace of CLFV is discovered, it will be a strong pillar to build the extension of SM.

4.3 Backgrounds to $\mu - e$ Conversion and Bound Muon Decay

The conversion experiments will measure the conversion ratio,

$$R_{\mu e} = \frac{\Gamma(\mu + N \to e + N)}{\Gamma(\mu + N \to \text{all muon captures})} \tag{4.2}$$

by detecting the momenta of the conversion electrons. There are three general backgrounds which are considered to put constraints on the beam structure, the detector types, and the required momentum resolution. The backgrounds are (1) intrinsic type (caused by the muons), (2) beam-related, and (3) cosmic type.

The muon decay in the atomic orbit of the target atom, also known as *decay in orbit*, (DIO), has the same time distribution as the conversion signal. Therefore, it is the most important intrinsic background and needs to be accounted carefully. It is imperative to

distinguish between the electrons from the weak decay of muonic atoms and the conversion electrons. Setting the appropriate momentum resolution from DIO calculation will guarantee it.

In the free muon decay, the momentum spectrum of the electron, also known as Michel spectrum [18], has an endpoint energy at

$$E_{max} = \frac{m_\mu^2 + m_e^2}{2m_\mu} = 52.8 \text{ MeV} \tag{4.3}$$

which can be derived from the conservation of four-momentum. The maximum energy for the conversion electron is the muon rest energy. Thus, the endpoint of muon-to-electron conversion is near 105.66 MeV (muon mass). Clearly, the free muon decay does not pose any background in a detector with modest resolution.

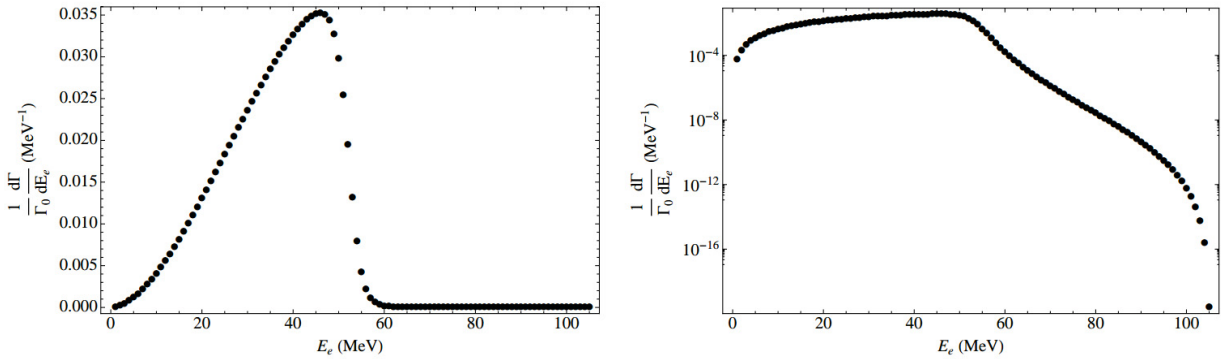

Figure 4.2: Electron energy spectrum for muon decay in orbit (aluminum nucleus) from [19]. Left plot is in linear scale, and right plot is in logarithmic scale.

On the other hand, DIO includes interaction of the electron with the nucleus exchanging a virtual photon. It can provide sufficient electron energy equivalent to the conversion energy. The detectors will observe free electrons, (both from conversion and DIO) recoiling from the nuclei. At the DIO end-point energy, neutrino energy is zero, recoiling decay electrons can have energy large enough that the detector may fail to distinguish them. DIO energy spectrum is shown in Fig. (4.2). There can be one event from DIO within less than 1 MeV of the conversion endpoint, which strengthens the probability of finding the desired conversion if $R_{\mu e} \sim 10^{-17}$.

Our investigation continues in bound muon decay. We study the decay behaviour of a bound muon into a bound electron. It has been recently found that the negative energy component of the bound muon wave function contributes significantly to this decay [3]. We explore this topic to understand how negative energy part of a bound state contributes to the decay process.

4.4 Conclusion

In this chapter, we summarized the essence of CLFV search and its experimental premises. Mu2e and COMET will run soon with its upgraded arrangement, and their findings can inform us to the right direction to pursue new physics. The problem of bound muon decay emerged as a dominant background of the conversion signal. DIO affirms that it is possible to discover CLFV if it exists within the lower bound sensitivity of the experimental settings.

Moreover, when analytically performed, the problem turned to be rich in interpretation. The bound-to-bound DIO has been the objective for this project. The decay result offers a new theoretical aspect of the negative energy part of a bound state. As for next action, we want to understand the underlying physics of the decay behaviour.

Chapter 5

The Ratio of Bound Muon and Free Muon Decay Rates

5.1 Introduction

Muon is the lightest unstable elementary particle. Its relatively long lifetime (2.2 μs) makes it an excellent probe to explore new physics beyond the Standard Model. A bound muon in a muonic atom can decay into a bound electron and neutrinos. This decay can be expressed as $(Z\mu^-) \to (Ze^-)\,\nu_\mu\bar{\nu}_e$ where (Zx^-) represents the bound atom. The decay rate is expressed as a single integral,

$$\frac{\Gamma\left((Z\mu^-) \to (Ze^-)\,\nu_\mu\bar{\nu}_e\right)}{\Gamma_0\left(\mu^- \to e^-\nu_\mu\bar{\nu}_e\right)} = 128\int_0^{z_{\max}} \left(N_a^2 + N_b^2 + F_a^2 + F_b^2\right) k_A z^3 dz, \tag{5.1}$$

as shown in [3] where $N_{a,b}$ and $F_{a,b}$ stand for spin non-flip and spin flip events of $\mu^- \to e^-$, Γ and Γ_0 are the bound muon and the free muon decay rates, respectively. z is a dimensionless variable characterizing the mass of a fictitious boson A, such that the decay can be broken up into two steps, $(Z\mu^-) \to (Ze^-)\,A$ and $A \to \nu_\mu\bar{\nu}_e$ with its mass, $m_A = zm_\mu$. z is maximum when the pair of neutrinos go in the opposite direction, and it is zero when they are in the same direction. The maximum value of z is given by $z_{\max} = \frac{E_\mu - E_e}{m_\mu}$, and the expressions of $N_{a,b}$ and $F_{a,b}$ are [3]

$$N_a = \sqrt{2}\frac{z_{\max}}{z}\left[4a^2\left(C_2 - S_3\right) + \left(1 + a^2\right)S_1\right], \tag{5.2}$$

$$N_b = \sqrt{2}\frac{k_A}{z}\left(1 + a^2\right)S_1, \tag{5.3}$$

$$F_a = 4a^2\left(C_2 - S_3\right) - 2\left(1 - a^2\right)S_1, \tag{5.4}$$

$$F_b = 4a\left(S_2 - C_1\right), \tag{5.5}$$

where

$$C_n = \frac{1+\gamma}{8}\left(\frac{4\delta}{(1+\delta)^2}\right)^{\gamma+\frac{1}{2}} \frac{\Gamma\left(1+2\gamma-n\right)}{k^n\Gamma\left(1+2\gamma\right)}\left(1+k^2\right)^{\frac{n-1}{2}-\gamma}\cos\left[\left(1+2\gamma-n\right)\arctan k\right], \tag{5.6}$$

and analogously S_n with $\cos \to \sin$. Other variables are defined as:

$$\alpha_Z = Z\alpha, \tag{5.7}$$

$$\gamma = \sqrt{1-\alpha_Z^2}, \tag{5.8}$$

$$a = \frac{1-\gamma}{\alpha_Z}, \tag{5.9}$$

$$k = \frac{k_A}{\alpha_Z\left(1+\delta\right)}, \tag{5.10}$$

$$k_A = \sqrt{z_{\max}^2 - z^2}, \tag{5.11}$$

$$z_{\max} = \frac{E_\mu - E_e}{m_\mu} = \frac{\gamma\left(m_\mu - m_e\right)}{m_\mu} = \gamma\left(1-\delta\right). \tag{5.12}$$

Here, E_i is the 1s binding energy of a Dirac particle of mass m_i in a hydrogenic atom, and $E_i = \gamma m_i$.

Binomial expansion in δ in Eq. [5.1],

$$\frac{\Gamma}{\Gamma_0} \propto \left(\left(\frac{\delta}{(1+\delta)^2}\right)^{\gamma+\frac{1}{2}}\right)^2 = \delta^{2\gamma+1}\left(1+\delta\right)^{-4\gamma-2} = \delta^{2\gamma+1} + \mathcal{O}\left(\delta^{2\gamma+2}\right) \to \delta^{2\gamma+1} \tag{5.13}$$

tells us that the leading order term in the δ-expansion of $\frac{\Gamma}{\Gamma_0}$ carries $\delta^{2\gamma+1}$. We shall factor this fractional power out in the expression of $\frac{\Gamma}{\Gamma_0}$. The plot of numerical values of $\frac{\Gamma}{\Gamma_0}\frac{1}{\delta^{2\gamma+1}}$ as a function of γ (setting $\delta = \frac{m_e}{m_\mu} = \frac{1}{207}$ in the rest of the expression) is illustrated in Fig. 5.1. $\frac{\Gamma}{\Gamma_0}$ vanishes at both ends, $\gamma = 0$ and 1 regardless of the directions of the neutrinos and the relative spin orientations of muon and electron. The physical reasons for this behaviour are explained in section 5.5.

However, we are interested in an analytic expression for $\frac{\Gamma}{\Gamma_0}$. Since δ is small from the definition ($\delta = \frac{m_e}{m_\mu} \ll 1$), we can take advantage of the smallness of this physical parameter to evaluate an asymptotic expression of $\frac{\Gamma}{\Gamma_0}$ as a function of δ and γ. This expression will tell us about the decay nature $\left(Z\mu^-\right) \to \left(Ze^-\right)\nu_\mu\bar{\nu}_e$, and thus, from the decay behaviour, we can draw an intuitive contrast between the corresponding decays in heavy atoms ($\alpha_Z \to 1$) and light atoms ($\alpha_Z \to 0$).

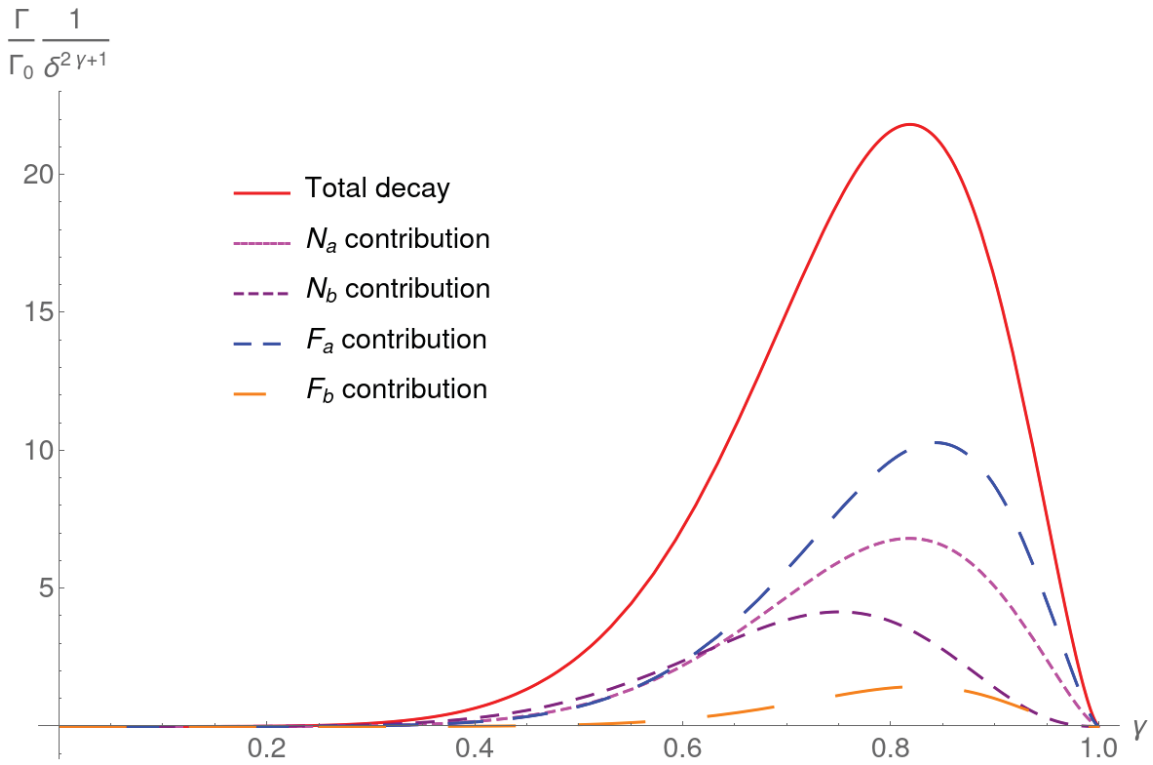

Figure 5.1: Plot of $\frac{\Gamma}{\Gamma_0}\frac{1}{\delta^{2\gamma+1}}$ with N_a, N_b, F_a, and F_b contributions.

As we have defined all the symbols and their meanings, we proceed with the integral in Eq. (5.1). We briefly explain how we can evaluate the integral approximately and calculate the asymptotic expression as $\gamma \to 0$ and $\gamma \to 1$. Then we present the approximate expression that is valid for all values of γ. In conclusion, we describe the vanishing nature of bound-to-bound decay in Section 5.5.

5.2 Procedure of Integration

In this section, we will simplify the integrand and convert it to a power series to perform the integration straight.

First we make a change of variables, $k(z) \to \tan\theta$ so that

$$C_n = \frac{1+\gamma}{8}\left(\frac{4\delta}{(1+\delta)^2}\right)^{\gamma+\frac{1}{2}} \frac{\Gamma(1+2\gamma-n)}{\Gamma(1+2\gamma)} \frac{(\sec\theta)^{n-1-2\gamma}}{\tan^n\theta} \cos\left[(1+2\gamma-n)\,\theta\right]. \tag{5.14}$$

The ratio of Gamma functions in Eq. (5.14) is expressed as a simple fraction,

$$\frac{\Gamma(1+2\gamma-n)}{\Gamma(1+2\gamma)} = \frac{\cancel{\Gamma(1+2\gamma-n)}}{(1+2\gamma-1)(1+2\gamma-2)...(1+2\gamma-n)\cancel{\Gamma(1+2\gamma-n)}}$$
$$= \frac{1}{(1+2\gamma-1)(1+2\gamma-2)...(1+2\gamma-n)}. \tag{5.15}$$

This exact fraction in (5.15) will be used for computational purpose.

We introduce a new parameter $\lambda = \alpha_Z(1+\delta)$ and

$$k = \frac{k_A}{\alpha_Z(1+\delta)} \Rightarrow k_A = \lambda \tan\theta. \tag{5.16}$$

Thus, we have the relation between z and θ variables,

$$k_A = \lambda\tan\theta \Rightarrow \sqrt{z_{\max}^2 - z^2} = \lambda\tan\theta. \tag{5.17}$$

From the last equation, we obtain new integration limits $\int_0^{z_{\max}} \to \int_{\theta_0}^0$ where $\theta_0 = \arctan\frac{z_{\max}}{\lambda}$. From Eq. (5.17), we get

$$z^2 = z_{\max}^2 - \lambda^2\tan^2\theta \Rightarrow zdz = -\lambda^2\tan\theta\sec^2\theta d\theta. \tag{5.18}$$

Let $f(\gamma,\delta,z) = 128\left(N_a^2 + N_b^2 + F_a^2 + F_b^2\right)k_A z^2$; then,

$$\frac{\Gamma}{\Gamma_0} = \int_0^{z_{\max}} f(\delta,\gamma,z)\,zdz = \int_{\theta_0}^0 f(\delta,\gamma,\theta)\times\left(-\lambda^2\tan\theta\sec^2\theta d\theta\right)$$

$$\frac{\Gamma}{\Gamma_0} \equiv \int_0^{\theta_0} G(\delta,\gamma,\theta)\,d\theta \tag{5.19}$$

where $G(\delta,\gamma,\theta)$ is the total integrand. Divergences can arise from C_n/S_n or $\tan\theta\sec^2\theta$ in the integrand at $\theta = \frac{\pi}{2}$. But $\frac{z_{\max}}{\alpha_Z(1+\delta)} < \infty \Rightarrow \theta_0 < \frac{\pi}{2}$, the integral will not have any divergence as $\frac{\pi}{2}$ fall outside the integration limit.

$G(\delta,\gamma,\theta)$ is a smooth function in the region $0 \le \theta \le \theta_0$; however, it is too complicated to give a compact integral. The principle to find an approximate expression for the integral Eq. (5.19) is to expand $G(\delta,\gamma,\theta)$ in a Taylor series of θ around $\theta = \theta' \in [0,\theta_0]$ and write $G(\delta,\gamma,\theta) = \sum_{n=0}^{\infty} c_n(\delta,\gamma)(\theta-\theta')^n$. This series can be simply integrated, since

$$\int_0^{\theta_0}(\theta-\theta')^n\,d\theta = \frac{(\theta_0-\theta')^{n+1} - (-\theta')^{n+1}}{n+1}. \tag{5.20}$$

Moreover, $G(\delta,\gamma,\theta)$ is an even function in θ i.e. $G(\delta,\gamma,-\theta) = G(\delta,\gamma,\theta)$. It can be shown

using the relations,

$$\begin{aligned} &\text{When } \theta \to -\theta, \\ &\quad C_n \to (-1)^n C_n, \\ &\quad S_n \to (-1)^{n+1} S_n, \\ &\quad k_A \to -k_A, \\ &\quad z \to z. \end{aligned}$$

Therefore, the Taylor expansion will have only the even powers of θ. In principle, we can write

$$\frac{\Gamma}{\Gamma_0} = \sum_{n=0,2,4}^{\infty} c_n(\delta,\gamma) \frac{(\theta_0 - \theta')^{n+1} - (-\theta')^{n+1}}{n+1}. \tag{5.21}$$

Eq. (5.21) is the key equation that yields us the decay ratio. The choice of θ' will decide where and how fast the series will converge. However, we can only take a finite number of terms in practice, and the more terms we include, the better approximation we obtain.

5.3 Asymptotic Behaviour as $\gamma \to 0$ and $\gamma \to 1$

First we will compute $\frac{\Gamma}{\Gamma_0}\frac{1}{\delta^{2\gamma+1}}$ as $\gamma \to 0$ and $\gamma \to 1$. Although it is a simple integral using the limit, one should be careful approximating the γ and θ-dependent integrand terms. We are looking for the coefficient of γ^n-like term (or α_Z^n), and if we substitute the limiting value for any γ-dependent integrand term (e.g. $\sin(2\gamma - 1)\theta$) in the calculation, sometimes we can miss a γ^n-contribution from the γ expansion of that particular term. It will provide a divergence in the calculation, even though the exact integral is finite.

When $\gamma \to 0$, we choose $\theta' = 0$ and take only the leading non-zero term in the RHS of Eq. (5.21). For $\gamma \to 1$, $\alpha_Z \to 0$; therefore, α_Z variable is used to find the asymptotic integral.

We find

$$\lim_{\gamma\to 0} \frac{\Gamma}{\Gamma_0}\frac{1}{\delta^{2\gamma+1}} = \frac{256}{15}\gamma^5, \tag{5.22}$$

$$\lim_{\gamma\to 1} \frac{\Gamma}{\Gamma_0}\frac{1}{\delta^{2\gamma+1}} = 96\pi\alpha_Z^3 = 96\pi\left(1-\gamma^2\right)^{\frac{3}{2}}. \tag{5.23}$$

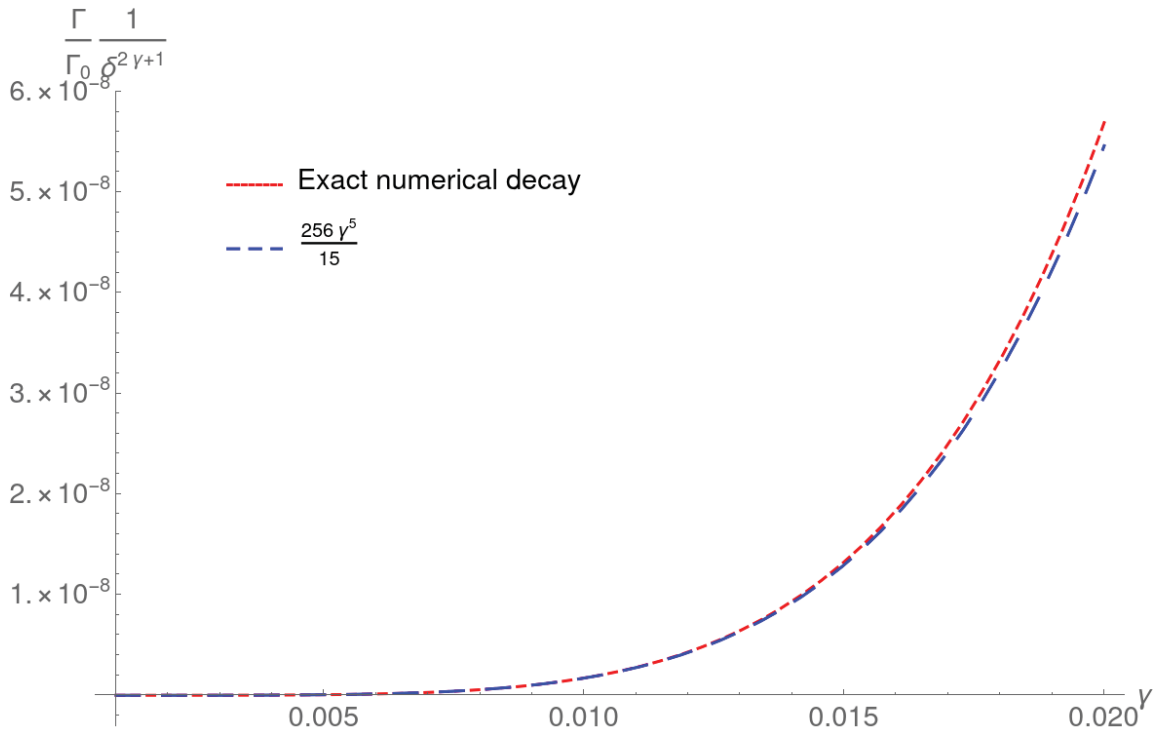

Figure 5.2: Plot of $\frac{\Gamma}{\Gamma_0}\frac{1}{\delta^{2\gamma+1}}$ and its asymptotic function as $\gamma \to 0$.

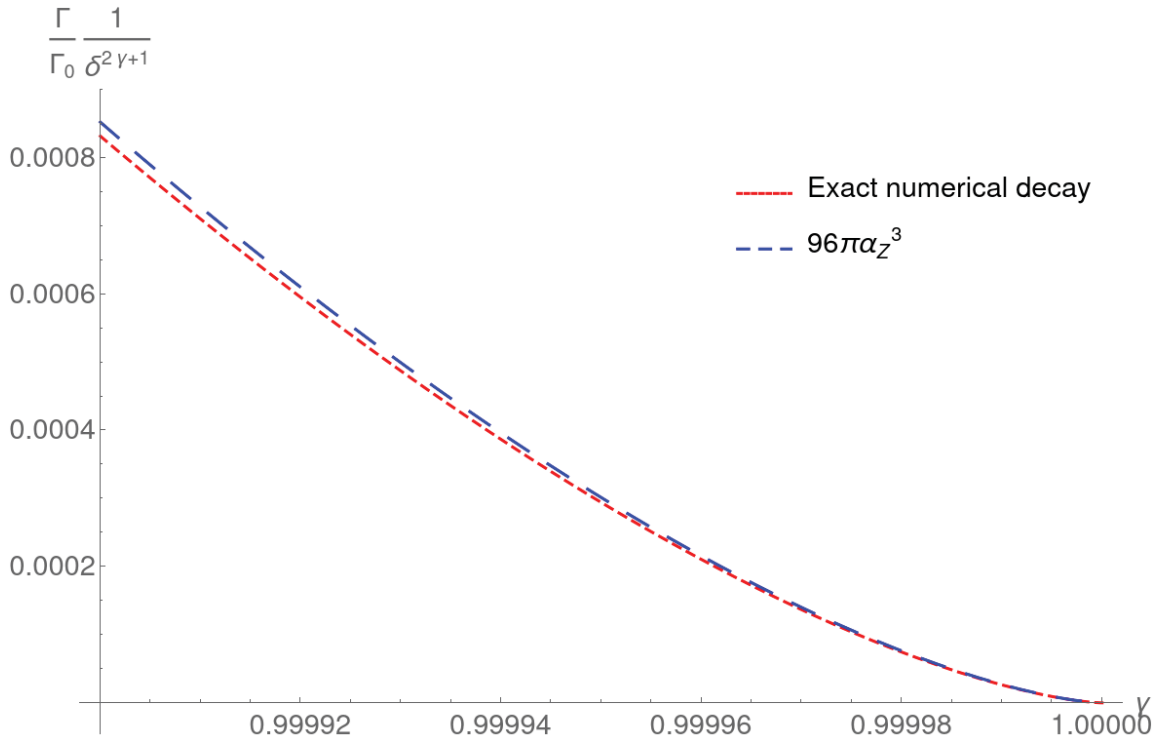

Figure 5.3: Plot of $\frac{\Gamma}{\Gamma_0}\frac{1}{\delta^{2\gamma+1}}$ and its asymptotic function as $\gamma \to 1$.

These results are calculated for the leading-order term of δ (as shown in Eq. (5.13)) taking advantage of the smallness of δ. We can conclude that the asymptotic terms in Eq. (5.22) and (5.23) are accurate comparing with the numerical result of Eq. (5.1) in Fig. 5.2 and Fig. 5.3, respectively.

5.4 Expression for $0 \leq \gamma \leq 1$

We will keep higher order terms in Eq. (5.21) to obtain an expression valid for all γ. Evidently, $\theta' = 0$ in Eq. (5.21) can produce the simplest expression of all choices of θ'. Setting $\theta' = 0$ in Eq. (5.21),

$$\frac{\Gamma}{\Gamma_0} \approx \sum_{n=0,2,4}^{16} c_n(\delta,\gamma)\frac{\theta_0^{n+1}}{n+1} \Rightarrow \frac{\Gamma}{\Gamma_0}\frac{1}{\delta^{2\gamma+1}} = 2^{5+4\gamma}\left(1-\gamma^2\right)^{3/2}\sum_{n=1,3}^{17} w(\delta,n,\gamma)\,\theta_0^n \tag{5.24}$$

where we changed the summation index $n \to n+1$, and $w(\delta,n,\gamma)$ is an $(n+1)$-order polynomial of γ. $n=3$ is the lowest order non-zero term, therefore θ_0^3 is factorized from all the terms.

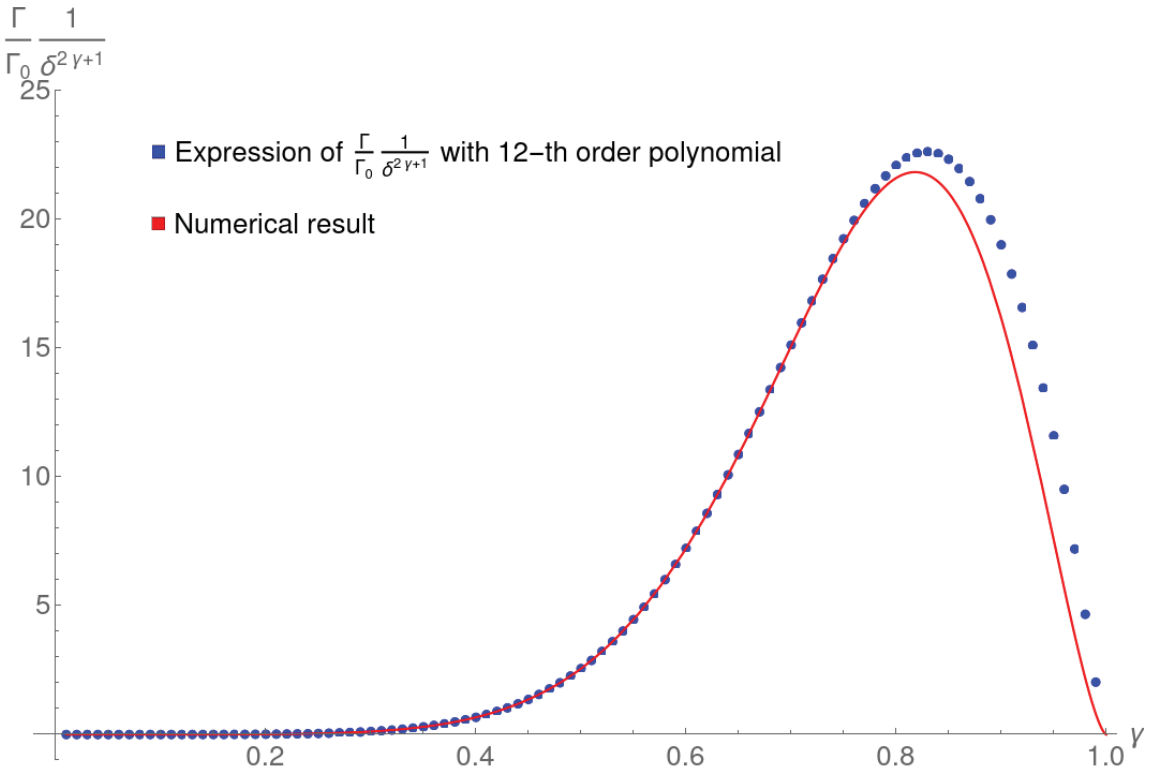

Figure 5.4: 12-order Taylor expansion of $f_0(\gamma) + f_1(\gamma)\,\delta$ in Eq. (5.26) does not fit the numerical result for large values of γ.

$$\frac{\Gamma}{\Gamma_0}\frac{1}{\delta^{2\gamma+1}} = 2^{5+4\gamma}\left(1-\gamma^2\right)^{3/2}\theta_0^3\sum_{n=0,2}^{14} w\left(\delta, n+3, \gamma\right)\theta_0^n \tag{5.25}$$

$$\Rightarrow \frac{\Gamma}{\Gamma_0}\frac{1}{\delta^{2\gamma+1}} \approx 2^{5+4\gamma}\alpha_Z^3\theta_0^3\left(f_0\left(\gamma\right)+\delta f_1\left(\gamma\right)\right) \tag{5.26}$$

In the last step, we made a δ-expansion as $\sum_{n=0,2}^{14} w\left(\delta, n+3, \gamma\right)\theta_0^n \approx f_0\left(\gamma\right)+f_1\left(\gamma\right)\delta+\mathcal{O}\left(\delta^2\right)$ and dropped $\mathcal{O}\left(\delta^2\right)$. Finally another Taylor expansion is performed on $f_0\left(\gamma\right)+f_1\left(\gamma\right)\delta$ around $\gamma = 0$ to produce a polynomial-like expression. The order of this polynomial determines how far the expression will be a good approximation.

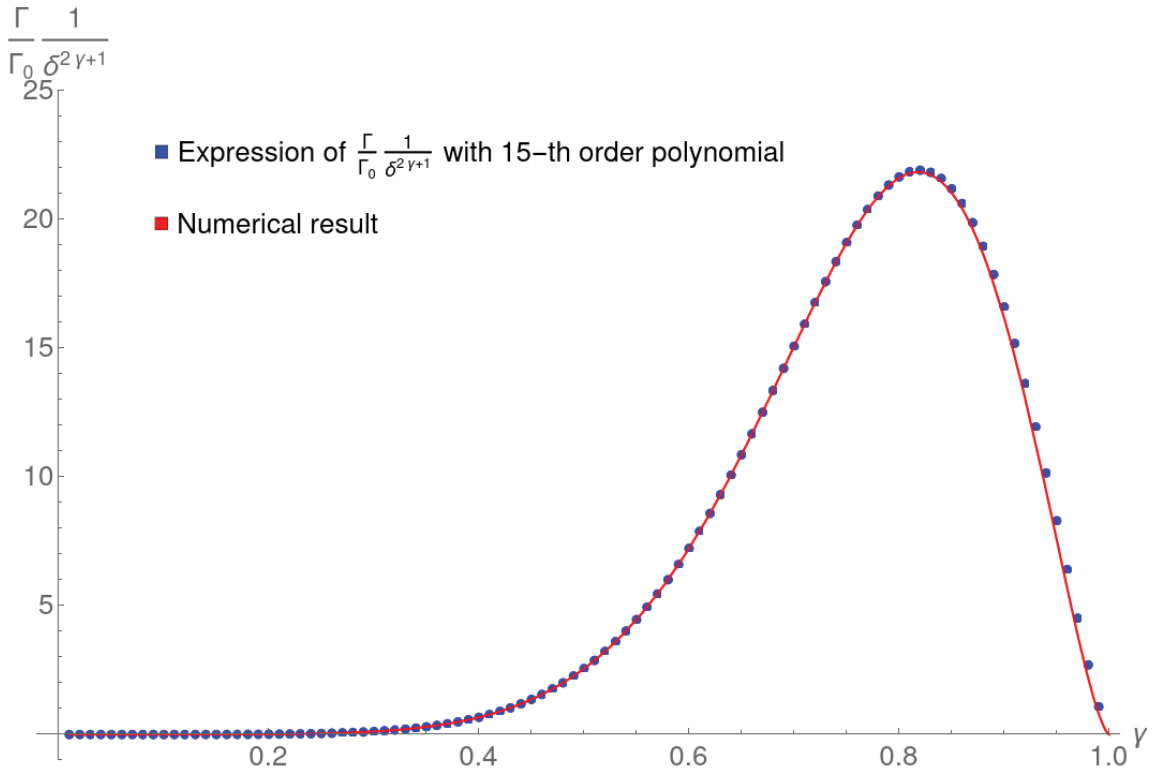

Figure 5.5: 15-order Taylor expansion of $f_0\left(\gamma\right)+f_1\left(\gamma\right)\delta$ in Eq. (5.26) fits the numerical result without any significant deviation.

Comparison between Fig. 5.4 and Fig. 5.5 illustrates that the 15-order Taylor expansion of $f_0\left(\gamma\right)+f_1\left(\gamma\right)\delta$ fits the numerical plot consistently. Furthermore, there is 0.5% difference at the peak point $\gamma \approx 0.83$ in Fig. 5.5. In Fig. 5.4, the difference is 4.1%. The order of polynomial is a matter of choice, and we choose it to be 15 to achieve a decent fit with fewer terms as possible.

Replacing $f_0\left(\gamma\right)+f_1\left(\gamma\right)\delta$ in Eq. (5.26) by a finite series expansion of order 15, we can

finally write,

$$
\begin{aligned}
f_0(\gamma)+f_1(\gamma)\,\delta = \frac{4\gamma^2}{32564156625}\big\{ & -4341887550(-1+\delta)-4341887550\gamma(-1+5\delta)\\
& -6822966150\gamma^2(-1+5\delta)-206756550\gamma^3(13+67\delta)\\
& +4594590\gamma^4(-727+6363\delta)+9189180\gamma^5(-1241+8033\delta)\\
& +2506140\gamma^6(-1537+21785\delta)+835380\gamma^7(-5671+16289\delta)\\
& -612\gamma^8(-9571451+91513537\delta)-153\gamma^9(-12459949+4244654 29\delta)\\
& -68\gamma^{10}(-109533853+848898624\delta)+136\gamma^{11}(-8351086+4626217\delta)\\
& +\gamma^{12}(3194531102+20768279230\delta)+\gamma^{13}(-4627628276+47663119216\delta)\big\}.
\end{aligned}
\tag{5.27}
$$

We can split this long expression into two expressions of arguments γ and α_Z respectively, that will match $\frac{\Gamma}{\Gamma_0}\frac{1}{\delta^{2\gamma+1}}$ from $\gamma=0$ and $\gamma=1\,(\alpha_Z=0)$ tails and meet in between (Fig. 5.6).

$$
f_0(\gamma)+f_1(\gamma)\,\delta = \begin{cases}
\alpha_Z^{12}(95.1\delta-5.02)+\alpha_Z^{10}(6.67-190.\delta)+\alpha_Z^{8}(186.\delta-0.945) & \text{upper tail}\\
+\alpha_Z^{6}(-88.1\delta-4.14)+\alpha_Z^{4}(19.3\delta+1.35)+\alpha_Z^{2}(0.509-1.14\delta) & \\
+(0.262-1.52\delta) & \\
 & \\
\frac{16\gamma^8(21785\delta-1537)}{51975}+\frac{16\gamma^7(8033\delta-1241)}{14175} & \text{lower tail}\\
+\frac{8\gamma^6(6363\delta-727)}{14175}-\frac{8}{315}\gamma^5(67\delta+13) & \\
-\frac{88}{105}\gamma^4(5\delta-1)-\frac{8}{15}\gamma^3(5\delta-1)-\frac{8}{15}\gamma^2(\delta-1) &
\end{cases}
\tag{5.28}
$$

All algebraic expressions and figures in this chapter have been produced using Mathematica [20].

Steps in Brief

Here I briefly go over the steps in the procedures explained in section [5.4]:

1. Approximation 1: $\theta'=0$ is used in Eq. (5.21) and the series is taken up to 16-th order terms.

2. After the integration, the integral is rearranged to write Eq. (5.25).

3. Approximation 2: We perform first order approximation of $\sum_{n=0,2}^{14} w(\delta,n+3,\gamma)\,\theta_0^n$ in δ-variable and produce Eq. (5.26).

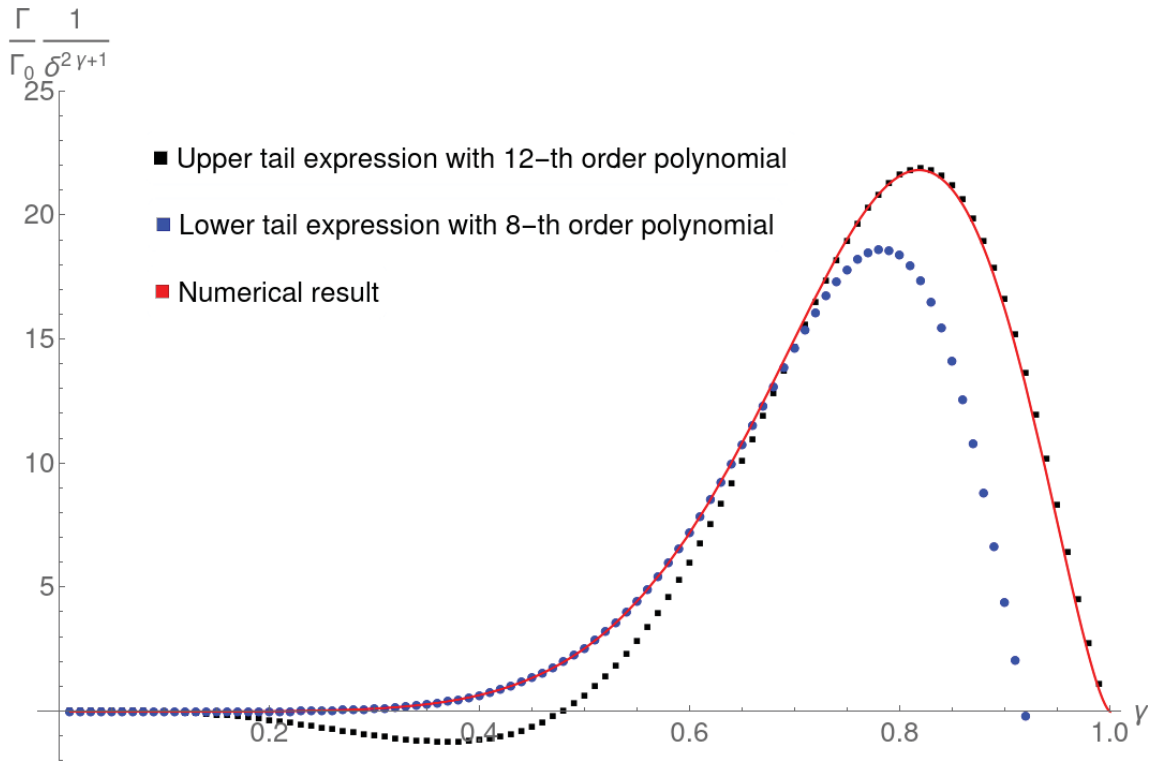

Figure 5.6: $\frac{\Gamma}{\Gamma_0}\frac{1}{\delta^{2\gamma+1}}$ from Eq. (5.26) is plotted with the 12-th order polynomial (upper tail) and 8-th order polynomial (lower tail) in Eq. (5.28). Both expressions are consistent with the numerical plot meeting around $\gamma \approx 0.7$.

4. Approximation 3: $f_0(\gamma) + f_1(\gamma)\,\delta$ is Taylor-expanded in δ to achieve a polynomial-like expression. 15-order polynomial is given by Eq. (5.27).

5. Eq. (5.27) is rearranged with respect to both end of γ values and a new form as in Eq. (5.28) is derived.

In summary, the exact analytic expression for the decay rate ratio is nearly impossible to achieve. We derived an approximate expression for $\frac{\Gamma}{\Gamma_0}\frac{1}{\delta^{2\gamma+1}}$ as a function of γ, and it fits the numerical plot. Therefore, the current formula given by Eq. (5.26) with Eq. (5.28) is an economic form to get the decay behaviour of bound muon to bound electron.

5.5 Interpretation

As depicted in Fig. 5.1, $\frac{\Gamma}{\Gamma_0}$ vanishes at $\gamma = 0$ and $\gamma = 1$. In this section, we will describe the vanishing behaviour physically.

We know, the energy of the bound particle is $E = \gamma m_i$ $(m_i = m_\mu, m_e)$. The difference of the energies of muon and electron is the energy of the neutrino pair, i.e., $E_\nu + E_{\bar{\nu}} = \gamma(m_\mu - m_e)$.

Large values of Z corresponds to $\gamma \to 0$, which implies the neutrino pair receives less energy from the decay as the atomic number Z increases. As the neutrino phase space gets smaller, the decay rate falls and becomes zero when the neutrino pair gets no energy from the decay.

For small values of Z, the phase space is larger. Regardless, the decay rate vanishes for $Z \to 0 \Leftrightarrow \gamma \to 1$. In fact, we can see from the numerical values of the derivatives of the asymptotic decay rate that $\frac{\Gamma}{\Gamma_0}$ drops faster near $\gamma = 1$ than $\gamma = 0$.

$$\text{For } \gamma \to 0: \quad \left.\frac{d\left(\frac{256\gamma^5}{15}\right)}{d\gamma}\right|_{\gamma=0.01} = 8.5 \times 10^{-7} \tag{5.29}$$

$$\text{For } \gamma \to 1: \quad \left.\frac{d\left(96\pi\left(1-\gamma^2\right)^{3/2}\right)}{d\gamma}\right|_{\gamma=0.99} = -126.36 \tag{5.30}$$

There must be a factor which causes $\frac{\Gamma}{\Gamma_0}$ to vanish near $\gamma = 1$ sharply. The bound muon to bound electron amplitude is,

$$\mathcal{M} = \frac{g}{\sqrt{2}} \int d^3r \exp(i\boldsymbol{q}.\boldsymbol{r}) \overline{\Phi}_e(\boldsymbol{r}) \not{\epsilon}^{\lambda_A *} L \Phi_\mu(\boldsymbol{r}) \tag{5.31}$$

where $\Phi_i(\boldsymbol{r})$ is the wave function of i particle (electron or muon), g is the weak interaction strength, $L = \frac{1-\gamma_5}{2}$. λ_A labels the polarization state of the boson A. The term $\exp(i\boldsymbol{q}.\boldsymbol{r})$ is the wave function for two neutrinos, where $\boldsymbol{q}$ is their total momentum. We consider the r-integral of $\mathcal{M}$ for 1s Dirac wave function,

$$\int_0^\infty dr\, r^{2\gamma} e^{-(m_\mu + m_e)\alpha_Z r} \exp(i\boldsymbol{q}.\boldsymbol{r}), \tag{5.32}$$

where $\boldsymbol{q}$ can have any magnitude from 0 to a maximum of $\gamma(m_\mu - m_e)$. We write $q = |\boldsymbol{q}| = \omega\gamma(m_\mu - m_e)$ where $0 \le \omega \le 1$, and make a change of variable $r \to x = (m_\mu + m_e)\alpha_Z r$. $\exp(i\boldsymbol{q}.\boldsymbol{r})$ can be rearranged as

$$\begin{aligned}
\exp(i\boldsymbol{q}.\boldsymbol{r}) &= \exp(iqr\cos\theta) \\
&= \exp(i\beta x \cos\theta) \\
&= \exp\left[\frac{\beta x}{2}\left(ie^{i\theta} - \frac{1}{ie^{i\theta}}\right)\right] \\
&= \sum_{n=-\infty}^{\infty} i^n e^{in\theta} J_n(\beta x)
\end{aligned} \tag{5.33}$$

where $\beta = \frac{\omega\gamma(m_\mu - m_e)}{(m_\mu + m_e)\alpha_Z} = \frac{\omega\gamma(1-\delta)}{\sqrt{1-\gamma^2}(1+\delta)}$. Here we identified the exponential function as the

generating function of Bessel functions of the first kind, $J_n(\beta x)$ [21] and expanded it in a Laurent series in Eq. (5.33). The r-integral in $\mathcal{M}$ becomes

$$\int_0^\infty dr\, r^{2\gamma} e^{-(m_\mu+m_e)\alpha_Z r} \exp(i\boldsymbol{q}.\boldsymbol{r}) \sim \sum_{n=-\infty}^{\infty} i^n e^{in\theta} \int_0^\infty dx\, x^{2\gamma} e^{-x} J_n(\beta x). \tag{5.34}$$

when $\gamma \to 1$, $\beta \to \infty$. In this limit, the asymptotic expression of $J_n(\beta x)$,

$$\begin{aligned}\lim_{\beta\to\infty} J_n(\beta x) =& \frac{1}{4\sqrt{2\pi}(\beta x)^{3/2}} \Bigg[(4n^2-1) \sin\left(\frac{1}{4}(2n+1)\pi - \beta x\right) \\ &+ 8\beta x \sin\left(\frac{1}{4}(2n-1)\pi + \beta x\right) \Bigg].\end{aligned} \tag{5.35}$$

In this limit, even for any small value of x, the asymptotic sinusoidal behaviour of $J_n(\beta x)$ becomes dominant. However, since $\alpha_Z \to 0$ in this limit and $x = (m_\mu + m_e)\alpha_Z r$, other factors of the r-dependent integrand ($x^{2\gamma}$ and e^{-x}) remain flat. The nature of asymptotic $J_n(\beta x)$ in Eq. [5.35] essentially determines the integral, and its positive and negative contributions from the sin functions cancel each other resulting a vanishing integral. To summarize, we can attribute this vanishing behaviour to the neutrino wave function $\exp(i\boldsymbol{q}.\boldsymbol{r})$ whose positive and negative components vanishes $\mathcal{M}$ as $\gamma \to 1$.

Intuitively, it might be tempting to convince oneself that the decay rate maintains a monotonic behaviour; but it does not. The neutrino phase space keeps shrinking as $\gamma \to 0$. As γ keeps increasing and goes to 1, the bound wave function spreads in the position space and becomes nearly flat. The oscillatory neutrino wave function cancels out with itself when multiplied with the uniformly-spread bound wave functions in the r integration. Together they vanish the decay rate at both ends.

5.6 Conclusion

The main result of the paper [3] was the single integral representation of the decay rate ratio as given in Eq. (5.1). The paper calculated the decay rate for the hypothetical case of $m_\mu \approx m_e$. In this chapter, we did not assume any artificial condition; but we have taken advantage of the smallness of the mass ratio $\delta = \frac{m_e}{m_\mu}$ by expanding parts of the integrand with respect to δ.

The bound-muon-to-bound-electron decay rate vanishes at $\gamma = 0$ since there is no energy left for the neutrinos from the decay. With the increase of γ, outgoing neutrinos are allowed to receive more energy, and the decay probability rises. However, the neutrino wave function is expressed by a series Bessel functions which exhibit oscillatory behaviour at large dis-

tance. The oscillatory neutrino wave coupled with the nearly-constant bound wave functions vanishes as we integrate over r in the position space.

As for the next step, we may study the decay of bound muon into free electron and connect with our interpretation. In that case, free electron wave function will be only oscillatory and can be merged with the neutrino wave function. In the bound electron case, there are two bound wave functions, combination of which made the bound part in the integrand nearly flat. For free decay electron, we have one muon bound wave function; therefore, it will be still flat. It motivates us to speculate that the decay rate still vanishes for free decay electron for $Z\alpha \to 0$.

Bibliography

[1] M. Lee, *COMET muon conversion experiment in J-PARC*, Frontiers in Physics **6**, 133 (2018).

[2] R. H. Bernstein, *The Mu2e experiment*, Frontiers in Physics **7**, 1 (2019).

[3] M. J. Aslam, A. Czarnecki, G. Zhang, and A. Morozova, *Decay of a bound muon into a bound electron*, Phys. Rev. D **102**, 073001 (2020).

[4] S. Kryuchkov, *On the one-photon annihilation of the Ps-ion*, Journal of Physics B: Atomic, Molecular and Optical Physics **27**, L61 (1994).

[5] V. Berestetskii, E. Lifshitz, and L. Pitaevskii, *Quantum Electrodynamics: Volume 4*, Course of theoretical physics, Elsevier Science (1982).

[6] A. P. Mills, *Observation of the positronium negative ion*, Phys. Rev. Lett. **46**, 717–720 (1981).

[7] D. B. Cassidy and A. Mills, *The production of molecular positronium*, Nature **449**, 195–197 (2007).

[8] J. Kuipers, T. Ueda, J. A. M. Vermaseren, and J. Vollinga, *FORM version 4.0*, Comput. Phys. Commun. **184**, 1453–1467 (2013), `1203.6543`.

[9] M. E. Peskin and D. V. Schroeder, *An Introduction to quantum field theory*, Addison-Wesley, Reading, USA (1995).

[10] A. H. Al-Ramadhan and D. W. Gidley, *New precision measurement of the decay rate of singlet positronium*, Phys. Rev. Lett. **72**, 1632–1635 (1994).

[11] J. A. Wheeler, *Polyelectrons*, Annals of the New York Academy of Sciences **48** (1946).

[12] A. M. Frolov, *Annihilation of electron-positron pairs in the positronium ion Ps^- and bipositronium Ps_2*, Phys. Rev. A **80**, 014502 (2009).

[13] J. Pérez-Ríos, S. T. Love, and C. H. Greene, *Two-photon total annihilation of molecular positronium*, EPL (Europhysics Letters) **109**, 63002 (2015).

[14] P. M. Platzman and A. P. Mills, *Possibilities for Bose condensation of positronium*, Phys. Rev. B **49**, 454–458 (1994).

[15] E. P. Hincks and B. Pontecorvo, *Search for gamma-radiation in the 2.2-microsecond meson decay process*, Phys. Rev. **73**, 257–258 (1948).

[16] A. de Gouvêa, *(Charged) lepton flavor violation*, Nuclear Physics B-Proceedings Supplements **188**, 303–308 (2009).

[17] W. J. Marciano, T. Mori, and J. M. Roney, *Charged Lepton Flavor Violation Experiments*, Ann. Rev. Nucl. Part. Sci. **58**, 315–341 (2008).

[18] L. Michel, *Interaction between four half-spin particles and the decay of the μ-meson*, Proceedings of the Physical Society. Section A **63**, 514 (1950).

[19] A. Czarnecki, X. Garcia i Tormo, and W. J. Marciano, *Muon decay in orbit: spectrum of high-energy electrons*, Phys. Rev. D **84**, 013006 (2011), `1106.4756`.

[20] Wolfram Research, Inc., *Mathematica, Version 12.1*, Champaign, IL, 2020.

[21] G. B. Arfken, H. J. Weber, and F. E. Harris, *Mathematical methods for physicists*, pages 643–713, Academic Press, Boston, 7th edition (2013).

Appendix A

Phase Space Integrals

A.1 Two Outgoing Photons

Let k_i the 4-momentum for the i-th photon. k_1^0 and k_2^0 are equal for symmetry. From Eq. (2.13), we can write

$$\int d\Pi_2 = \int \frac{d^3k_1}{(2\pi)^3 2k_1^0}\frac{d^3k_2}{(2\pi)^3 2k_2^0}(2\pi)^4\delta^4(p_A - k_1 - k_2) \tag{A.1}$$

$$= (2\pi)^{-2}\int \frac{d^3k_1}{2k_1^0}\frac{d^3k_2}{2k_2^0}\delta^4(p_A - k_1 - k_2) \tag{A.2}$$

$$= \frac{1}{4\pi^2}\int \frac{d^3k_1}{4k_1^2}\delta(p_A^0 - 2k_1^0) \quad (k_2^0 = k_1^0) \tag{A.3}$$

$$= \frac{1}{2}\frac{1}{16\pi^2}\int d\Omega \int dk_1 \delta(k_1 - \frac{p_A^0}{2}) \quad (k_1^0 = |\boldsymbol{k}_1| = k_1) \tag{A.4}$$

$$= \frac{1}{32\pi^2}\int d\Omega \tag{A.5}$$

$$= \frac{1}{8\pi} \tag{A.6}$$

Eq. (A.6) is used in the two-photon annihilations in Chapter 2 and 3.

A.2 One Electron and One Photon

Let p and E stand for 4-momentum and energy while their subscript labels γ and f are for the photon and the electron. The energy-momentum relations are $E_\gamma = p_\gamma$ and $E_f = \sqrt{p_f^2 + m^2}$. The phase space integral is,

$$\int d\Pi_2 = \int \frac{d^3p_\gamma}{(2\pi)^3 2E_\gamma}\frac{d^3p_f}{(2\pi)^3 2E_f}(2\pi)^4\delta^4(p_A - p_f - p_\gamma) \tag{A.7}$$

$$= \frac{1}{4\pi^2}\frac{1}{4}\int \frac{d^3p_\gamma}{p_\gamma}\frac{p_f^2 dp_f d\Omega_f}{\sqrt{p_f^2+m^2}}\delta^4(p_A - p_f - p_\gamma) \tag{A.8}$$

$$= \frac{1}{4\pi^2}\frac{1}{4}\int \frac{1}{p_f}\times\frac{p_f^2 dp_f d\Omega_f}{\sqrt{p_f^2+m^2}}\delta(p_A^0 - \sqrt{p_f^2+m^2} - p_f) \quad (p_\gamma = |\boldsymbol{p}_f| = p_f) \tag{A.9}$$

$$= \frac{1}{4\pi^2}\frac{1}{4}\int \frac{p_f dp_f d\Omega_f}{\sqrt{p_f^2+m^2}}\delta(p_A^0 - \sqrt{p_f^2+m^2} - p_f). \tag{A.10}$$

Now on, p_A^0 will be denoted by p_A. The root of the argument of the delta function is $p_A - \sqrt{p_f^2+m^2} - p_f = 0 \Rightarrow p_f = \frac{p_A^2-m^2}{2p_A}$.

$$\frac{d}{dp_f}\left(p_A - \sqrt{p_f^2+m^2} - p_f\right)_{p_f=\frac{p_A^2-m^2}{2p_A}} = -\frac{2p_A^2}{p_A^2+m^2} \tag{A.11}$$

$$\therefore \delta(p_A - \sqrt{p_f^2+m^2} - p_f) = \frac{\delta(p_f - \frac{p_A^2-m^2}{2p_A})}{\left|-\frac{2p_A^2}{p_A^2+m^2}\right|} = \frac{p_A^2+m^2}{2p_A^2}\delta(p_f - \frac{p_A^2-m^2}{2p_A}) \tag{A.12}$$

$$\int d\Pi_2 = \frac{1}{4\pi^2}\frac{1}{4}\int d\Omega_f \int \frac{p_f dp_f}{\sqrt{p_f^2+m^2}}\delta(p_A - \sqrt{p_f^2+m^2} - p_f) \tag{A.13}$$

$$= \frac{1}{4\pi^2}\frac{1}{4}\times 4\pi \times \frac{p_A^2+m^2}{2p_A^2}\int \frac{p_f dp_f}{\sqrt{p_f^2+m^2}}\delta(p_f - \frac{p_A^2-m^2}{2p_A}) \tag{A.14}$$

$$= \frac{1}{4\pi}\frac{p_A^2+m^2}{2p_A^2}\frac{\left(\frac{p_A^2-m^2}{2p_A}\right)}{\frac{p_A^2+m^2}{2p_A}} \tag{A.15}$$

$$= \frac{1}{4\pi}\frac{1}{p_A}\left(\frac{p_A^2-m^2}{2p_A}\right) \tag{A.16}$$

Putting $p_A = 3m$ (as in Ps^- ion),

$$\int d\Pi_2 = \frac{1}{9\pi}. \tag{A.17}$$

Eq. (A.17) is used in the single photon annihilation in Chapter 2.

Appendix B

Symmetry Factor for Incoming Identical Particles

Identical particles in the initial state contribute a symmetry factor $\frac{1}{n!}$ to the scattering amplitude where n is the number of identical particles of a single type. In the outgoing state, the amplitude has the same factor from the phase space integral which is intuitive to understand. However, $\frac{1}{n!}$ from the initial state non-trivially arises from normalization of the initial state and the commutator algebra of the creation and annihilation operators of the identical particles. In this appendix, first we will explain how we can write a bound state generally, and then we will recover the symmetry factor from the normalization of the bound state.

Note that initial state may not be strictly a bound state, nonetheless we are able to write it in the same manner as we will write the bound state generally in B.1. Therefore, the symmetry factor derived here holds for all cases.

B.1 Expression of the Bound State $|B\rangle$

A free particle is described by the state $|\boldsymbol{k}\rangle$ with the normalization,

$$\langle \boldsymbol{k}' \,|\, \boldsymbol{k}\rangle = (2\pi)^3 \delta^3(\boldsymbol{k}' - \boldsymbol{k}). \tag{B.1}$$

An open system of n free particles, where particles can exchange energy among themselves and with any external agent, can be similarly given by the state $|\boldsymbol{k}_1, ..., \boldsymbol{k}_n\rangle$ satisfying

$$\langle \boldsymbol{k}'_1, ..., \boldsymbol{k}'_n \,|\, \boldsymbol{k}_1, ..., \boldsymbol{k}_n\rangle = \prod_{i=1}^{n} (2\pi)^3 \delta^3(\boldsymbol{k}'_i - \boldsymbol{k}_i). \tag{B.2}$$

Total energy and momentum is not conserved in an open system. Let's consider a bound state $|B(\boldsymbol{P},\sigma_B,\sigma)\rangle$ with a total momentum $\boldsymbol{P}$ ($\boldsymbol{P}=\sum_i \boldsymbol{k}_i$) and where $\sigma_B(\sigma_B+1)$ and σ are the $\hat{S}^2$ and $\hat{S}_3$ eigenvalues. Normalization of such a bound state is

$$\langle B(\boldsymbol{P}',\sigma_B',\sigma')\,|\,B(\boldsymbol{P},\sigma_B,\sigma)\rangle = (2\pi)^3\delta^3(\boldsymbol{P}'-\boldsymbol{P})\delta_{\sigma_B'\sigma_B}\delta_{\sigma'\sigma}. \tag{B.3}$$

We can write $|B(\boldsymbol{P},\sigma_B,\sigma)\rangle$ as a superposition of all momentum states of all the particles. We may choose to write the superposition as

$$|B(\boldsymbol{P},\sigma_B,\sigma)\rangle \sim \prod_{i=1}^{n}\sum_{\sigma_i}\sum_{\boldsymbol{k}_i}\psi_{\sigma_1...\sigma_n}(\boldsymbol{k}_1,...,\boldsymbol{k}_n)\delta_{\sigma,\sigma_1+...+\sigma_n}\hat{O}_{\sigma_1...\sigma_n}(\boldsymbol{k}_1,...,\boldsymbol{k}_n)\,|0\rangle\,. \tag{B.4}$$

The operator $\hat{O}_{\sigma_1...\sigma_n}(\boldsymbol{k}_1,...,\boldsymbol{k}_n)$ creates i th particle of $\boldsymbol{k}_i$ momentum and σ_i 3-spin. ψ is a wave function describing how the particles are constrained in this bound state of total spin σ where $\delta_{\sigma,\sigma_1+...+\sigma_n}$ on the right hand side maintains the 3-spin conservation as we sum over σ_i. The summations $\sum_{\boldsymbol{k}_i}$ and $\sum_{\sigma_i}$ include all momenta and spins; we can replace the $\boldsymbol{k}$ summations as $\sum_{\boldsymbol{k}_i}\to\int\frac{d^3\boldsymbol{k}_i}{(2\pi)^3}$ where $(2\pi)^3$ is a conventional factor. All these integrals are required to respect the total momentum $\boldsymbol{P}$ on the left hand side of [B.4] i.e. $\boldsymbol{P}=\sum_i\boldsymbol{k}_i$. It is guaranteed by the inclusion of a delta function $\delta^3(\boldsymbol{P}-\boldsymbol{k}_1-\boldsymbol{k}_2...-\boldsymbol{k}_n)$ inside the integrals $\int\frac{d^3\boldsymbol{k}_i}{(2\pi)^3}$. Moreover, specifying the total 3-spin σ_i demands appropriate Clebsch-Gordan coefficients (denoted as $c^{(\sigma_B)}_{\sigma;\sigma_1...\sigma_n}$) on the right hand side which substitute spin-conservation $\delta_{\sigma,\sigma_1+...+\sigma_n}$ term. We will denote the Clebsch-Gordan coefficients [1] as $c^{(\sigma_B)}_{\sigma;\sigma_1...\sigma_n}$ for $|\sigma_B,\sigma\rangle = |s_1,\sigma_1\rangle\oplus...\oplus|s_n,\sigma_n\rangle$. Therefore, the bound state is *defined* as

$$\begin{aligned}|B(\boldsymbol{P},\sigma_B,\sigma)\rangle \equiv \prod_{i=1}^{n}\sum_{\sigma_i}\int\frac{d^3\boldsymbol{k}_i}{(2\pi)^3}(2\pi)^3\delta^3(\boldsymbol{P}-\boldsymbol{k}_1-\boldsymbol{k}_2-...-\boldsymbol{k}_n)c^{(\sigma_B)}_{\sigma;\sigma_1...\sigma_n}\psi_{\sigma_1...\sigma_n}(\boldsymbol{k}_1,...,\boldsymbol{k}_n)\\ \times\hat{O}_{\sigma_1...\sigma_n}(\boldsymbol{k}_1,...,\boldsymbol{k}_n)\,|0\rangle\,.\end{aligned} \tag{B.5}$$

We have included another conventional factor $(2\pi)^3$ with $\delta^3(\boldsymbol{P}-\boldsymbol{k}_1-\boldsymbol{k}_2-...-\boldsymbol{k}_n)$, any arbitrary factor will be absorbed into ψ to preserve the normalization in [B.3]. We may

[1] In the bound state, there can be more than two angular momenta as $|\sigma_B,\sigma\rangle = |s_1,\sigma_1\rangle\oplus...\oplus|s_n,\sigma_n\rangle$ where s_i and σ_i are the spin and the 3-spin of i th particle. Therefore, $|B\rangle$ will have more than two Casimir operators ($\hat{S}^2$ and $\hat{S}_3$) and thus we will need more than two labels (σ_B,σ). We should keep that in mind while calculating for arbitrary bound state. For now, we look over other eigenvalues from other possible Casimir operators and carry out the general expression because this choice does not affect our result.

re-write Eq. (B.5) as

$$|B(\boldsymbol{P},\sigma_B,\sigma)\rangle = \prod_{i=1}^{n}\sum_{\sigma_i}\int \frac{d^3\boldsymbol{k}_i}{(2\pi)^3} c^{(\sigma_B)}_{\sigma;\sigma_1\ldots\sigma_n}\Psi_{\sigma_1\ldots\sigma_n}(\boldsymbol{P};\boldsymbol{k}_1,...,\boldsymbol{k}_n)\hat{O}_{\sigma_1\ldots\sigma_n}(\boldsymbol{k}_1,...,\boldsymbol{k}_n)\,|0\rangle \quad \text{(B.6)}$$

where

$$\Psi_{\sigma_1\ldots\sigma_n}(\boldsymbol{P};\boldsymbol{k}_1,...,\boldsymbol{k}_n) = (2\pi)^3\delta^3(\boldsymbol{P}-\boldsymbol{k}_1-\boldsymbol{k}_2-...-\boldsymbol{k}_n)\psi_{\sigma_1\ldots\sigma_n}(\boldsymbol{k}_1,...,\boldsymbol{k}_n). \quad \text{(B.7)}$$

B.2 Symmetry Factor from the Normalization of a Bound State

We will consider the bound state of Ps^- ion that contains two identical electron (fermions). We will show that it requires a factor of $\frac{1}{2}$ to preserve the normalization. Analyzing the same calculation, we can convince ourselves that of a factor of $\frac{1}{n!}$ for n identical fermions and bosons.

Eq. (B.6) and [B.7] motivates us to write,

$$\begin{aligned}\left|\mathrm{Ps}^-(\boldsymbol{P},\sigma_B,\sigma)\right\rangle = &\sum_{\sigma_i}\int \frac{d^3\boldsymbol{k}_1}{(2\pi)^3}\frac{d^3\boldsymbol{k}_2}{(2\pi)^3}\frac{d^3\boldsymbol{k}_3}{(2\pi)^3} c^{(\sigma_B)}_{\sigma;\sigma_1\sigma_2\sigma_3}\Psi_{\sigma_1\sigma_2\sigma_3}(\boldsymbol{P};\boldsymbol{k}_1,\boldsymbol{k}_2,\boldsymbol{k}_3)\\ &\times a^\dagger_{\sigma_1}(\boldsymbol{k}_1)a^\dagger_{\sigma_2}(\boldsymbol{k}_2)b_{\sigma_3}(\boldsymbol{k}_3)|0\rangle\end{aligned}$$

where $a_\sigma(\boldsymbol{k})$ annihilates an electron of spin σ and momentum $\boldsymbol{k}$, and $b_\sigma(\boldsymbol{k})$ creates a positron of spin σ and momentum $\boldsymbol{k}$.

$$\begin{aligned}&\langle \mathrm{Ps}^-(\boldsymbol{P}',\sigma_B,\sigma)|\mathrm{Ps}^-(\boldsymbol{P},\sigma_B,\sigma)\rangle\\ &= \sum_{\sigma_i'}\sum_{\sigma_i} c^{(\sigma_B)}_{\sigma;\sigma_1'\sigma_2'\sigma_3'}c^{(\sigma_B)}_{\sigma;\sigma_1\sigma_2\sigma_3}\int\frac{d^3\boldsymbol{k}_1'}{(2\pi)^3}\frac{d^3\boldsymbol{k}_2'}{(2\pi)^3}\frac{d^3\boldsymbol{k}_3'}{(2\pi)^3}\int\frac{d^3\boldsymbol{k}_1}{(2\pi)^3}\frac{d^3\boldsymbol{k}_2}{(2\pi)^3}\frac{d^3\boldsymbol{k}_3}{(2\pi)^3}\\ &\times \Psi^*_{\sigma_1'\sigma_2'\sigma_3'}(\boldsymbol{P}';\boldsymbol{k}_1',\boldsymbol{k}_2',\boldsymbol{k}_3')\Psi_{\sigma_1\sigma_2\sigma_3}(\boldsymbol{P};\boldsymbol{k}_1,\boldsymbol{k}_2,\boldsymbol{k}_3)\\ &\times \langle 0|\, b^\dagger_{\sigma_3'}(\boldsymbol{k}_3')a_{\sigma_2'}(\boldsymbol{k}_2')a_{\sigma_1'}(\boldsymbol{k}_1')a^\dagger_{\sigma_1}(\boldsymbol{k}_1)a^\dagger_{\sigma_2}(\boldsymbol{k}_2)b_{\sigma_3}(\boldsymbol{k}_3)\,|0\rangle\end{aligned} \quad \text{(B.8)}$$

We use the following anti-commutative relations,

$$\left\{a_{\sigma'}(\boldsymbol{k}'),a^\dagger_\sigma(\boldsymbol{k})\right\} = \left\{b_{\sigma'}(\boldsymbol{k}'),b^\dagger_\sigma(\boldsymbol{k})\right\} = (2\pi)^3\delta_{\sigma\sigma'}\delta^3(\boldsymbol{k}-\boldsymbol{k}'), \quad \text{(B.9)}$$

$$\{a_{\sigma'}(\boldsymbol{k}'),a_\sigma(\boldsymbol{k})\} = \{b_{\sigma'}(\boldsymbol{k}'),b_\sigma(\boldsymbol{k})\} = \left\{a_{\sigma'}(\boldsymbol{k}'),b^\dagger_\sigma(\boldsymbol{k})\right\} = 0, \quad \text{(B.10)}$$

to evaluate the product of the operators in $\langle \mathrm{Ps}^-(\boldsymbol{P}', \sigma_B, \sigma)|\mathrm{Ps}^-(\boldsymbol{P}, \sigma_B, \sigma)\rangle$.

$$
\begin{aligned}
& b^\dagger_{\sigma_3'}(\boldsymbol{k}_3')a_{\sigma_2'}(\boldsymbol{k}_2')a_{\sigma_1'}(\boldsymbol{k}_1')a^\dagger_{\sigma_1}(\boldsymbol{k}_1)a^\dagger_{\sigma_2}(\boldsymbol{k}_2)b_{\sigma_3}(\boldsymbol{k}_3) \\
=& \left(\left\{b^\dagger_{\sigma_3'}(\boldsymbol{k}_3'), b_{\sigma_3}(\boldsymbol{k}_3)\right\} - b_{\sigma_3}(\boldsymbol{k}_3)b^\dagger_{\sigma_3'}(\boldsymbol{k}_3')\right) \\
& \times \left(a_{\sigma_2'}(\boldsymbol{k}_2')\left\{a_{\sigma_1'}(\boldsymbol{k}_1'), a^\dagger_{\sigma_1}(\boldsymbol{k}_1)\right\}a^\dagger_{\sigma_2}(\boldsymbol{k}_2) - a_{\sigma_2'}(\boldsymbol{k}_2')a^\dagger_{\sigma_1}(\boldsymbol{k}_1)a_{\sigma_1'}(\boldsymbol{k}_1')a^\dagger_{\sigma_2}(\boldsymbol{k}_2)\right) \\
=& \left\{b^\dagger_{\sigma_3'}(\boldsymbol{k}_3'), b_{\sigma_3}(\boldsymbol{k}_3)\right\}\left\{a_{\sigma_1'}(\boldsymbol{k}_1'), a^\dagger_{\sigma_1}(\boldsymbol{k}_1)\right\}a_{\sigma_2'}(\boldsymbol{k}_2')a^\dagger_{\sigma_2}(\boldsymbol{k}_2) \\
& - b_{\sigma_3}(\boldsymbol{k}_3)\left\{a_{\sigma_1'}(\boldsymbol{k}_1'), a^\dagger_{\sigma_1}(\boldsymbol{k}_1)\right\}a_{\sigma_2'}(\boldsymbol{k}_2')a^\dagger_{\sigma_2}(\boldsymbol{k}_2)b^\dagger_{\sigma_3'}(\boldsymbol{k}_3') \\
& - \left\{b^\dagger_{\sigma_3'}(\boldsymbol{k}_3'), b_{\sigma_3}(\boldsymbol{k}_3)\right\}a_{\sigma_2'}(\boldsymbol{k}_2')a^\dagger_{\sigma_1}(\boldsymbol{k}_1)a_{\sigma_1'}(\boldsymbol{k}_1')a^\dagger_{\sigma_2}(\boldsymbol{k}_2) \\
& + b_{\sigma_3}(\boldsymbol{k}_3)a_{\sigma_2'}(\boldsymbol{k}_2')a^\dagger_{\sigma_1}(\boldsymbol{k}_1)a_{\sigma_1'}(\boldsymbol{k}_1')a^\dagger_{\sigma_2}(\boldsymbol{k}_2)b^\dagger_{\sigma_3'}(\boldsymbol{k}_3') \\
=& \left\{b^\dagger_{\sigma_3'}(\boldsymbol{k}_3'), b_{\sigma_3}(\boldsymbol{k}_3)\right\}\left\{a_{\sigma_1'}(\boldsymbol{k}_1'), a^\dagger_{\sigma_1}(\boldsymbol{k}_1)\right\}\left\{a_{\sigma_2'}(\boldsymbol{k}_2'), a^\dagger_{\sigma_2}(\boldsymbol{k}_2)\right\} \\
& - \left\{b^\dagger_{\sigma_3'}(\boldsymbol{k}_3'), b_{\sigma_3}(\boldsymbol{k}_3)\right\}\left\{a_{\sigma_1'}(\boldsymbol{k}_1'), a^\dagger_{\sigma_1}(\boldsymbol{k}_1)\right\}a^\dagger_{\sigma_2}(\boldsymbol{k}_2)a_{\sigma_2'}(\boldsymbol{k}_2') \\
& - \left\{b^\dagger_{\sigma_3'}(\boldsymbol{k}_3'), b_{\sigma_3}(\boldsymbol{k}_3)\right\}\left(\left\{a_{\sigma_2'}(\boldsymbol{k}_2'), a^\dagger_{\sigma_1}(\boldsymbol{k}_1)\right\} - a^\dagger_{\sigma_1}(\boldsymbol{k}_1)a_{\sigma_2'}(\boldsymbol{k}_2')\right) \\
& \times \left(\left\{a_{\sigma_1'}(\boldsymbol{k}_1'), a^\dagger_{\sigma_2}(\boldsymbol{k}_2)\right\} - a^\dagger_{\sigma_2}(\boldsymbol{k}_2)a_{\sigma_1'}(\boldsymbol{k}_1')\right) \\
=& \left\{b^\dagger_{\sigma_3'}(\boldsymbol{k}_3'), b_{\sigma_3}(\boldsymbol{k}_3)\right\}\left\{a_{\sigma_1'}(\boldsymbol{k}_1'), a^\dagger_{\sigma_1}(\boldsymbol{k}_1)\right\}\left\{a_{\sigma_2'}(\boldsymbol{k}_2'), a^\dagger_{\sigma_2}(\boldsymbol{k}_2)\right\} \\
& - \left\{b^\dagger_{\sigma_3'}(\boldsymbol{k}_3'), b_{\sigma_3}(\boldsymbol{k}_3)\right\}\left\{a_{\sigma_2'}(\boldsymbol{k}_2'), a^\dagger_{\sigma_1}(\boldsymbol{k}_1)\right\}\left\{a_{\sigma_1'}(\boldsymbol{k}_1'), a^\dagger_{\sigma_2}(\boldsymbol{k}_2)\right\} \\
=& \delta_{\sigma_1\sigma_1'}\delta_{\sigma_2\sigma_2'}\delta_{\sigma_3\sigma_3'}(2\pi)^3\delta^3(\boldsymbol{k}_3 - \boldsymbol{k}_3')(2\pi)^3\delta^3(\boldsymbol{k}_1 - \boldsymbol{k}_1')(2\pi)^3\delta^3(\boldsymbol{k}_2 - \boldsymbol{k}_2') \\
& - \delta_{\sigma_1\sigma_2'}\delta_{\sigma_2\sigma_1'}\delta_{\sigma_3\sigma_3'}(2\pi)^3\delta^3(\boldsymbol{k}_3 - \boldsymbol{k}_3')(2\pi)^3\delta^3(\boldsymbol{k}_2 - \boldsymbol{k}_1')(2\pi)^3\delta^3(\boldsymbol{k}_1 - \boldsymbol{k}_2') \qquad \text{(B.11)}
\end{aligned}
$$

where all the terms with a or $b^\dagger$ on the right-most position are dropped because $a\,|0\rangle = b^\dagger\,|0\rangle = 0$.

Therefore,

$$
\begin{aligned}
& \langle \mathrm{Ps}^-(\boldsymbol{P}')|\mathrm{Ps}^-(\boldsymbol{P})\rangle \\
=& \sum_{\sigma_i'}\sum_{\sigma_i} c^{(\sigma_B)\,*}_{\sigma;\sigma_1'\sigma_2'\sigma_3'}c^{(\sigma_B)}_{\sigma;\sigma_1\sigma_2\sigma_3}\int\frac{d^3\boldsymbol{k}_1'}{(2\pi)^3}\frac{d^3\boldsymbol{k}_2'}{(2\pi)^3}\frac{d^3\boldsymbol{k}_3'}{(2\pi)^3}\int\frac{d^3\boldsymbol{k}_1}{(2\pi)^3}\frac{d^3\boldsymbol{k}_2}{(2\pi)^3}\frac{d^3\boldsymbol{k}_3}{(2\pi)^3} \\
& \times \Psi^*_{\sigma_1'\sigma_2'\sigma_3'}(\boldsymbol{P}';\boldsymbol{k}_1',\boldsymbol{k}_2',\boldsymbol{k}_3')\Psi_{\sigma_1\sigma_2\sigma_3}(\boldsymbol{P};\boldsymbol{k}_1,\boldsymbol{k}_2,\boldsymbol{k}_3) \\
& \times \langle 0|\, b^\dagger_{\sigma_3'}(\boldsymbol{k}_3')a_{\sigma_2'}(\boldsymbol{k}_2')a_{\sigma_1'}(\boldsymbol{k}_1')a^\dagger_{\sigma_1}(\boldsymbol{k}_1)a^\dagger_{\sigma_2}(\boldsymbol{k}_2)b_{\sigma_3}(\boldsymbol{k}_3)\,|0\rangle
\end{aligned}
$$

$$
\begin{aligned}
=&\sum_{\sigma_i'}\sum_{\sigma_i} c^{(\sigma_B)*}_{\sigma;\sigma_1'\sigma_2'\sigma_3'} c^{(\sigma_B)}_{\sigma;\sigma_1\sigma_2\sigma_3} \int \frac{d^3\boldsymbol{k}_1'}{(2\pi)^3}\frac{d^3\boldsymbol{k}_2'}{(2\pi)^3}\frac{d^3\boldsymbol{k}_3'}{(2\pi)^3} \int \frac{d^3\boldsymbol{k}_1}{(2\pi)^3}\frac{d^3\boldsymbol{k}_2}{(2\pi)^3}\frac{d^3\boldsymbol{k}_3}{(2\pi)^3} \\
&\times \Psi^*_{\sigma_1'\sigma_2'\sigma_3'}(\boldsymbol{P}';\boldsymbol{k}_1',\boldsymbol{k}_2',\boldsymbol{k}_3')\Psi_{\sigma_1\sigma_2\sigma_3}(\boldsymbol{P};\boldsymbol{k}_1,\boldsymbol{k}_2,\boldsymbol{k}_3) \\
&\times \Big\{ \delta_{\sigma_1\sigma_1'}\delta_{\sigma_2\sigma_2'}\delta_{\sigma_3\sigma_3'}(2\pi)^3\delta^3(\boldsymbol{k}_3-\boldsymbol{k}_3')(2\pi)^3\delta^3(\boldsymbol{k}_1-\boldsymbol{k}_1')(2\pi)^3\delta^3(\boldsymbol{k}_2-\boldsymbol{k}_2') \\
&- \delta_{\sigma_1\sigma_2'}\delta_{\sigma_2\sigma_1'}\delta_{\sigma_3\sigma_3'}(2\pi)^3\delta^3(\boldsymbol{k}_3-\boldsymbol{k}_3')(2\pi)^3\delta^3(\boldsymbol{k}_2-\boldsymbol{k}_1')(2\pi)^3\delta^3(\boldsymbol{k}_1-\boldsymbol{k}_2') \Big\} \\
=&\sum_{\sigma_i}\int \frac{d^3\boldsymbol{k}_1}{(2\pi)^3}\frac{d^3\boldsymbol{k}_2}{(2\pi)^3}\frac{d^3\boldsymbol{k}_3}{(2\pi)^3} \Big\{ \left|c^{(\sigma_B)}_{\sigma;\sigma_1\sigma_2\sigma_3}\right|^2 \Psi^*_{\sigma_1\sigma_2\sigma_3}(\boldsymbol{P}';\boldsymbol{k}_1,\boldsymbol{k}_2,\boldsymbol{k}_3) \\
&- c^{(\sigma_B)*}_{\sigma;\sigma_2\sigma_1\sigma_3} c^{(\sigma_B)}_{\sigma;\sigma_1\sigma_2\sigma_3} \Psi^*_{\sigma_2\sigma_1\sigma_3}(\boldsymbol{P}';\boldsymbol{k}_2,\boldsymbol{k}_1,\boldsymbol{k}_3) \Big\} \Psi_{\sigma_1\sigma_2\sigma_3}(\boldsymbol{P};\boldsymbol{k}_1,\boldsymbol{k}_2,\boldsymbol{k}_3)
\end{aligned} \tag{B.12}
$$

The wave function,

$$
\sum_{\sigma_i} c^{(\sigma_B)}_{\sigma;\sigma_1\sigma_2\sigma_3}\Psi_{\sigma_1\sigma_2\sigma_3}(\boldsymbol{P};\boldsymbol{k}_1,\boldsymbol{k}_2,\boldsymbol{k}_3) = f(\boldsymbol{P};\boldsymbol{k}_1,\boldsymbol{k}_2,\boldsymbol{k}_3)\sum_{\sigma_i} c^{(\sigma_B)}_{\sigma;\sigma_1\sigma_2\sigma_3}\chi_{\sigma_1\sigma_2\sigma_3} \tag{B.13}
$$

is anti-symmetric for $1 \leftrightarrow 2$ where $\chi_{\sigma_1\sigma_2\sigma_3}$ is the normalized spin wave function labeled with the 3-spin eigenvalues, and $\sum_{\sigma_i} c^{(\sigma_B)}_{\sigma;\sigma_1\sigma_2\sigma_3}\chi_{\sigma_1\sigma_2\sigma_3}$ is the total spin wave function for $\left|\mathrm{Ps}^-(\boldsymbol{P},\sigma_B,\sigma)\right\rangle$. f is the momentum-dependent scalar function that can be taken out of the summation. If f is symmetric for $1 \leftrightarrow 2$, $\sum_{\sigma_i} c^{(\sigma_B)}_{\sigma;\sigma_1\sigma_2\sigma_3}\chi_{\sigma_1\sigma_2\sigma_3}$ is anti-symmetric i.e. $c^{(\sigma_B)}_{\sigma;\sigma_1\sigma_2\sigma_3} = -c^{(\sigma_B)}_{\sigma;\sigma_2\sigma_1\sigma_3}$ and vice versa. Regardless of which component is anti-symmetric, we can safely write

$$
c^{(\sigma_B)*}_{\sigma;\sigma_2\sigma_1\sigma_3}\Psi^*_{\sigma_2\sigma_1\sigma_3}(\boldsymbol{P}';\boldsymbol{k}_2,\boldsymbol{k}_1,\boldsymbol{k}_3) = -c^{(\sigma_B)*}_{\sigma;\sigma_1\sigma_2\sigma_3}\Psi^*_{\sigma_1\sigma_2\sigma_3}(\boldsymbol{P}';\boldsymbol{k}_1,\boldsymbol{k}_2,\boldsymbol{k}_3). \tag{B.14}
$$

Thus, Eq. (B.12) reduces to

$$
\begin{aligned}
&\langle \mathrm{Ps}^-(\boldsymbol{P}')|\mathrm{Ps}^-(\boldsymbol{P})\rangle \\
=&\sum_{\sigma_i}\int \frac{d^3\boldsymbol{k}_1}{(2\pi)^3}\frac{d^3\boldsymbol{k}_2}{(2\pi)^3}\frac{d^3\boldsymbol{k}_3}{(2\pi)^3} \Big\{ \left|c^{(\sigma_B)}_{\sigma;\sigma_1\sigma_2\sigma_3}\right|^2 \Psi^*_{\sigma_1\sigma_2\sigma_3}(\boldsymbol{P}';\boldsymbol{k}_1,\boldsymbol{k}_2,\boldsymbol{k}_3) \\
&+ c^{(\sigma_B)*}_{\sigma;\sigma_1\sigma_2\sigma_3} c^{(\sigma_B)}_{\sigma;\sigma_1\sigma_2\sigma_3} \Psi^*_{\sigma_1\sigma_2\sigma_3}(\boldsymbol{P}';\boldsymbol{k}_2,\boldsymbol{k}_1,\boldsymbol{k}_3) \Big\} \Psi_{\sigma_1\sigma_2\sigma_3}(\boldsymbol{P};\boldsymbol{k}_1,\boldsymbol{k}_2,\boldsymbol{k}_3) \\
=&2\sum_{\sigma_i}\int \frac{d^3\boldsymbol{k}_1}{(2\pi)^3}\frac{d^3\boldsymbol{k}_2}{(2\pi)^3}\frac{d^3\boldsymbol{k}_3}{(2\pi)^3} \left|c^{(\sigma_B)}_{\sigma;\sigma_1\sigma_2\sigma_3}\right|^2 \Psi^*_{\sigma_1\sigma_2\sigma_3}(\boldsymbol{P}';\boldsymbol{k}_1,\boldsymbol{k}_2,\boldsymbol{k}_3)\Psi_{\sigma_1\sigma_2\sigma_3}(\boldsymbol{P};\boldsymbol{k}_1,\boldsymbol{k}_2,\boldsymbol{k}_3)
\end{aligned}
$$

$$
\begin{aligned}
=&2\sum_{\sigma_i}\int \frac{d^3\boldsymbol{k}_1}{(2\pi)^3}\frac{d^3\boldsymbol{k}_2}{(2\pi)^3}\frac{d^3\boldsymbol{k}_3}{(2\pi)^3}\left|c^{(\sigma_B)}_{\sigma;\sigma_1\sigma_2\sigma_3}\right|^2(2\pi)^3\delta^{(3)}(\boldsymbol{P}'-\boldsymbol{k}_1-\boldsymbol{k}_2-\boldsymbol{k}_3)\psi^*_{\sigma_1\sigma_2\sigma_3}(\boldsymbol{k}_1,\boldsymbol{k}_2,\boldsymbol{k}_3)\\
&(2\pi)^3\delta^{(3)}(\boldsymbol{P}-\boldsymbol{k}_1-\boldsymbol{k}_2-\boldsymbol{k}_3)\psi_{\sigma_1\sigma_2\sigma_3}(\boldsymbol{k}_1,\boldsymbol{k}_2,\boldsymbol{k}_3)\\
=&2(2\pi)^3\delta^{(3)}(\boldsymbol{P}-\boldsymbol{P}')\sum_{\sigma_i}\int \frac{d^3\boldsymbol{k}_1}{(2\pi)^3}\frac{d^3\boldsymbol{k}_2}{(2\pi)^3}\left|c^{(\sigma_B)}_{\sigma;\sigma_1\sigma_2\sigma_3}\psi_{\sigma_1\sigma_2\sigma_3}(\boldsymbol{k}_1,\boldsymbol{k}_2,\boldsymbol{P}-\boldsymbol{k}_1-\boldsymbol{k}_2)\right|^2. \qquad \text{(B.15)}
\end{aligned}
$$

As $\psi_{\sigma_1\sigma_2\sigma_3}(\boldsymbol{k}_1,\boldsymbol{k}_2,\boldsymbol{P}-\boldsymbol{k}_1-\boldsymbol{k}_2)\equiv\psi_{\sigma_1\sigma_2\sigma_3}(\boldsymbol{P};\boldsymbol{k}_1,\boldsymbol{k}_2)$, the final expression becomes

$$
\begin{aligned}
&\langle \mathrm{Ps}^-(\boldsymbol{P}',\sigma_B,\sigma)|\mathrm{Ps}^-(\boldsymbol{P},\sigma_B,\sigma)\rangle\\
=&2(2\pi)^3\delta^{(3)}(\boldsymbol{P}-\boldsymbol{P}')\sum_{\sigma_i}\int \frac{d^3\boldsymbol{k}_1}{(2\pi)^3}\frac{d^3\boldsymbol{k}_2}{(2\pi)^3}\left|c^{(\sigma_B)}_{\sigma;\sigma_1\sigma_2\sigma_3}\psi_{\sigma_1\sigma_2\sigma_3}(\boldsymbol{P};\boldsymbol{k}_1,\boldsymbol{k}_2)\right|^2. \qquad \text{(B.16)}
\end{aligned}
$$

It is evident that the normalization of the bound state $|\mathrm{Ps}^-\rangle$ comes with this additional factor of two which has to be compensated to retain the normalization of the state as given in Eq. (B.3). This is the reason to add a factor of $\frac{1}{2}$ in the decay expression of $\mathrm{Ps}^-\to e^-\gamma$ attributed to the identical electrons.

In general, if there were n identical fermions in a state $|B\rangle$, there are $n!$ ways to pair up the annihilation and creation operators in anti-commutators. The product of operators will have terms of both signs present as we saw in Eq. (B.11). (+)-signed terms are derived after getting even number of anti-commutators in the expression, and (−)-signed terms for any odd number. Antisymmetricity of the wave function compensates the − sign as for any odd number of exchange in fermions, the total state holds a negative sign. Therefore, we have $n!$ terms contributing the same quantity. In the normalization of the state, $n!$ comes out of the expression,

$$
\begin{aligned}
&\langle B(\boldsymbol{P}',\sigma_B,\sigma)|B(\boldsymbol{P},\sigma_B,\sigma)\rangle\\
=&n!(2\pi)^3\delta^{(3)}(\boldsymbol{P}-\boldsymbol{P}')\prod_{i=1}^{n}\sum_{\sigma_i}\int \frac{d^3\boldsymbol{k}_i}{(2\pi)^3}\left|c^{(\sigma_B)}_{\sigma;\sigma_1\sigma_2\ldots\sigma_n}\psi_{\sigma_1\sigma_2\ldots\sigma_n}(\boldsymbol{P};\boldsymbol{k}_1,\boldsymbol{k}_2,\ldots,\boldsymbol{k}_n)\right|^2. \qquad \text{(B.17)}
\end{aligned}
$$

The same procedure holds for identical bosons as well. Bosons will satisfy commutative relation,

$$
\left[a_{\sigma'}(\boldsymbol{k}'),a^\dagger_\sigma(\boldsymbol{k})\right]=\left[b_{\sigma'}(\boldsymbol{k}'),b^\dagger_\sigma(\boldsymbol{k})\right]=(2\pi)^3\delta_{\sigma\sigma'}\delta^3(\boldsymbol{k}-\boldsymbol{k}'), \qquad \text{(B.18)}
$$

$$
[a_{\sigma'}(\boldsymbol{k}'),a_\sigma(\boldsymbol{k})]=[b_{\sigma'}(\boldsymbol{k}'),b_\sigma(\boldsymbol{k})]=\left[a_{\sigma'}(\boldsymbol{k}'),b^\dagger_\sigma(\boldsymbol{k})\right]=0. \qquad \text{(B.19)}
$$

Therefore, the minus sign in Eq. (B.11) will be plus for the bosons in the initial state, and consequently, the normalization term will have a plus sign unlike Eq. (B.12). Since bosons will form a symmetric wave function, all the terms will be added and the factor $n!$ will arise

from the addition if there are n identical bosons.

To preserve the normalization of the initial state, we divide the final expression by $n!$. Thus comes the rule of $\frac{1}{n!}$ factor for any n number of identical particles in the initial state. The origin of this factor is the operator algebra of the identical particles; fermions and bosons both will have the factor respecting the spin-statistics theorem.